A New Species of Stream-Breeding Isthmohyla (Anura: Hylidae) from Costa Rica

Authors: Chaves-Acuña, Wagner, Abarca, Juan, Navarro-Picado, Jonathan, Hidalgo-Mora, Esteban, Ureña-Chaves, Marilyn, et al.

Source: Ichthyology & Herpetology, 114(2) : 337-356

Published By: The American Society of Ichthyologists and Herpetologists

URL: https://doi.org/10.1643/h2024066

Ichthyology & Herpetology 114, No. 2, 2026, 337–356

A New Species of Stream-Breeding *Isthmohyla* (Anura: Hylidae) from Costa Rica

Wagner Chaves-Acuña[1,2], Juan Abarca[3,4], Jonathan Navarro-Picado[5,6], Esteban Hidalgo-Mora[7], Marilyn Ureña-Chaves[6], Alejandro Valverde-Castillo[8], Gerardo Chaves[9], Federico Bolaños[9,10], and Julián Faivovich[1,2]

We describe a new species of the *Isthmohyla tica* group that occurs along the montane regions of the central Pacific of Costa Rica, between 1,400 and 2,000 masl. Although the new species is the sister taxon of a clade including an undescribed species and *I. rivularis*, it is more similar to *I. tica*. However, the new species can be distinguished because the flanks have scattered, distinct, round and irregular dark blotches or spots and because the advertisement call is comprised by a single, tonal note, typically emitted singly or in series, at dominant frequencies of 4,048–4,909 Hz, with a duration of 10–50 ms. The new species exhibits a broad acoustic repertoire composed of advertisement, release, and courtship calls, with the latter being emitted underwater. We discuss our findings with respect to adult and larval morphology, reproductive biology, and bioacoustics of the *I. tica* group.

ISTHMOHYLA is a hylid genus that comprises 13 species endemic to the isthmian highlands of Central America, ranging from the northernmost portion of the Cordillera de Guanacaste in northern Costa Rica to the easternmost end of the Serranía de Tabasará in western Panama (Duellman, 1970, 2001; Faivovich et al., 2018; Chaves-Acuña et al., 2024; Frost, 2026). Species in this genus inhabit a wide range of habitats including bromeliads, ponds, and fast- and slow-moving streams (Duellman, 1970, 2001). The genus comprises two major clades: one including the *I. pseudopuma* group (*I. infucata* and *I. pseudopuma*) and the *I. zeteki* group (*I. picadoi* and *I. zeteki*), and the other with the *I. tica* group. The latter includes nine species, two of which are associated with lentic environments (*I. angustilineata* and *I. graceae*) and seven species that are associated with riparian habitats (*I. calypsa*, *I. debilis*, *I. lancasteri*, *I. pictipes*, *I. rivularis*, *I. tica*, and *I. xanthosticta*). Four species (*I. angustilineata*, *I. calypsa*, *I. pictipes*, and *I. xanthosticta*) have not been available for phylogenetic analyses and are included in the *I. tica* group based on previous studies that indicated similarities with other species in the group (Duellman, 1970, 2001; Myers and Duellman, 1982; Lips, 1996; Faivovich et al., 2005, 2018).

Recent fieldwork in the northwestern part of the Cordillera de Talamanca, central Pacific of Costa Rica, in a region locally known as Los Santos, has led to the discovery of a new stream-breeding species from the *Isthmohyla tica* group, initially misidentified as the nominal species in previous studies (Duellman, 1970; Savage, 2002; Hidalgo-Mora et al., 2022). In this paper, we describe the new species along with its tadpoles and vocalizations, and we discuss its conservation status across its distribution.

MATERIALS AND METHODS

Adult morphology.—Adult specimens were euthanized with benzocaine, fixed in 10% formalin, and stored in 70% ethanol. The specimens are housed in the Museo de Zoología, Universidad de Costa Rica (UCR) and in the collection of amphibians of the Museo de Zoología, Escuela de Biología, Universidad Nacional de Costa Rica (ECBAnf). Webbing formula follows Savage and Heyer (1967) as modified by Myers and Duellman (1982). The standard terms for snout shape

[1] División Herpetología, Museo Argentino de Ciencias Naturales "Bernardino Rivadavia"–Consejo Nacional de Investigaciones Científicas y Técnicas, Ángel Gallardo 470, C1405DJR, Buenos Aires, Argentina; ORCID: (WCA) 0000-0002-6669-5701; and (JF) 0000-0001-7157-8131; Email: (WCA) wchaves512@gmail.com; and (JF) jfaivovich@gmail.com. Send correspondence to JF.
[2] Departamento de Biodiversidad y Biología Experimental, Facultad de Ciencias Exactas y Naturales, Universidad de Buenos Aires, Buenos Aires, Argentina.
[3] Alianza Nacional para la Conservación de Anfibios y Reptiles (ANCAR), Alajuela 20106, Costa Rica; ORCID: 0000-0002-1261-4400; Email: barcazajuan@gmail.com.
[4] Unidad de Microbiología Médico Veterinaria, Servicio Nacional de Salud Animal, Heredia, Costa Rica.
[5] Instituto Internacional de Conservación y Manejo de Vida Silvestre (ICOMVIS), Universidad Nacional, Heredia, Costa Rica; ORCID: 0000-0003-3380-9546; Email: jon90np@gmail.com.
[6] Escuela de Ciencias Biológicas, Universidad Nacional, Heredia, Costa Rica; ORCID: (MUC) 0009-0004-5711-9755; Email: (MUC) milyn30uch@gmail.com.
[7] Laboratorio de Ecología Funcional y Ecosistemas Tropicales, Escuela de Ciencias Biológicas, Universidad Nacional, Heredia, Costa Rica; ORCID: 0000-0002-3502-6660; Email: jairohm.9@gmail.com.
[8] Laboratorio de Patología Experimental y Comparada, Escuela de Biología, Universidad de Costa Rica, San José, Costa Rica; ORCID: 0009-0007-6857-187X; Email: valverde7740@gmail.com.
[9] Museo de Zoología, Centro de Investigaciones en Biodiversidad y Ecología Tropical, Universidad de Costa Rica, 11501-2060, Montes de Oca, San José, Costa Rica; ORCID: (GC) 0000-0002-4301-6569; and (FB) 0000-0002-7935-6418; Email: (GC) cachi13@gmail.com; and (FB) federico.bolanos@ucr.ac.cr.
[10] Escuela de Biología, Universidad de Costa Rica, 11501-2060, Montes de Oca, San José, Costa Rica.
Submitted: 30 July 2024. Accepted: 23 November 2025. Associate Editor: T. Grande.
 DOI: 10.1643/h2024066 Published online: 3 July 2026

are those of Duellman (1970); for nuptial pad structure, those of Luna et al. (2018); and for tympanum structure, those of Lynch and Duellman (1980). Finger numbering from II to V follows Fabrezi and Alberch (1996). We obtained 15 measurements using a digital caliper under a stereomicroscope, rounded to the nearest 0.1 mm. Measurements follow the standards of Duellman (1970): SVL (snout–vent length), HL (head length), HW (head width), IND (internarial distance), IOD (interorbital distance), ED (eye diameter), TD (tympanum diameter), END (eye–nostril distance), TL (tibia length), and FL (foot length). The diameter of the disc on the fourth finger of the hand (4FD) and the fourth toe of the foot (4TD) follow Napoli and Caramaschi (1998). Forearm length (FAL), thigh length (THL), and snout length (SL) follow Watters et al. (2016). Sex was determined by examination of secondary sexual characters (nuptial pads and expansion of the vocal sac) or by the visibility of eggs through the skin of the belly and flanks.

Observations in captivity.—Due to the limited knowledge of the reproductive biology of most riparian species of *Isthmohyla*, we conducted a four-day observation of courtship behaviors of an adult male (UCR 24367) and a gravid female (UCR 24368). These observations took place in a terrarium measuring 80 × 80 × 60 cm (width × depth × height), including 30 cm water depth, rocks, and overhanging vegetation.

Vocalizations.—Recordings were done with a Tascam DR-40x recorder and unidirectional Sennheiser ME 66 microphone positioned at about 1–3 m from the calling individuals. Calls were recorded at a sampling rate of 44.1 kHz and a 16-bit resolution. We deposited digital copies of audio files in Fonoteca Neotropical Jacques Vielliard (https://www2.ib.unicamp.br/fnjv/; Universidade Estadual de Campinas, Campinas, Sao Paulo, Brazil; FNJV 124945–56). We measured spectral and temporal parameters using Raven Pro 1.6.1 (Cornell Lab of Ornithology) with the following settings: window type Hann, window size of 512 samples, 3 dB filter bandwidth of 124 Hz, 50% overlap, hop size of 256 samples, DFT size of 512 samples, and grid spacing at 86.1 Hz. Figures were produced with seewave v. 1.7.6 (Sueur et al., 2008) in R 4.0.2 (R Core Team, 2020), using the following settings: window = Hanning, FFT overlap = 90%, FFT size = 512 points. Spectrograms were produced with a relative amplitude color scale of 30 dB (red = maximum amplitude). Calls were described using the terminology of Köhler et al. (2017), considering the following parameters: call duration, intercall duration, call envelope, minimum and maximum frequency, dominant frequency, and amplitude and frequency modulation. We used the definition of 'call' as a unit of vocalization, which is separated from other calls by an intercall interval (silent period) that is longer than the call duration (Köhler et al., 2017). Oscillograms were used to manually obtain the number of calls per call series and to determine if calls were pulsed or pulsatile. Oscillograms were also used to calculate the call duration (s) and the intercall interval (s) using the "Delta time" function of Raven. We also described the amplitude modulation of calls considering the presence of amplitude peaks throughout the call duration. We estimated the call rate within a call series as the number of calls divided by the call series duration. Spectrograms were used to obtain dominant frequency (Hz), minimum frequency (Hz), and maximum frequency (Hz) values using the "Peak frequency," "Frequency 5%," and "Frequency 95%" functions, respectively.

Tadpole morphology.—Tadpoles were collected using dip nets, euthanized in a 5% lidocaine solution, and preserved in 5% formalin. For species identification, we preserved tissue samples in 96% ethanol. A commercial solution of methylene blue was applied topically to enhance contrast where needed, particularly to better visualize the marginal and submarginal papillae. The terminology employed for the description is that of Duellman (1970), Altig and McDiarmid (1999a), and Pezzuti et al. (2021). We obtained 22 measurements (in millimeters, rounded to the nearest 0.1 mm) with the aid of a digital caliper or an Olympus DP22 camera attached to an Olympus SZX16 stereoscope following Altig and McDiarmid (1999b) for total length (TL), body length (BL), tail length (TAL), maximum tail height (MTH), internostril distance (IND), interorbital distance (IOD), tail muscle height (TMH), and tail muscle width (TMW); Lavilla and Scrocchi (1986) for body width (BW), body width at level of nostrils (BWN), body width at eye level (BWE), body height (BH), eye–nostril distance (END), nostril–snout distance (NSD), eye diameter (ED), nostril diameter (ND), snout–spiracle distance (SSD), and oral disc width (ODW); Grosjean (2005) for dorsal fin height (DFH) and ventral fin height (VFH); Lins et al. (2018) for spiracle length (SL), and spiracular–venter distance (SVD). We followed Gosner (1960) to classify larval developmental stages.

Comparisons with other species.—We studied preserved adult and larval specimens from UCR, Museo Herpetológico de Chiriquí, Universidad Autónoma de Chiriquí (MHCH), Círculo Herpetológico de Panama (CH), Instituto Conmemorativo Gorgas de Estudios de la Salud (ICGES), Natural History Museum of Los Angeles County (LACM), and the University of Kansas (KU). Comparisons of coloration in life and vocalizations were made based on recent findings of species of the *Isthmohyla tica* group, except for *I. calypsa* and *I. xanthosticta*. We also analyzed audio recordings obtained from the acoustic repositories of the Macaulay Library, University of Cornell (ML) and the American Museum of Natural History (AMNH).

DNA sequencing and analysis.—Whole cellular DNA was extracted from ethanol-preserved tissues (liver or muscle) using either phenol-chloroform extraction, salt precipitation methods, or the DNeasy tissue kit (Qiagen Inc.). We produced sequences of three mitochondrial genes, 12–16S RNA, NADH ubiquinone oxidoreductase 1 and their intervening tRNA (tRNA-Val and tRNA-Leu), and nuclear gene fragments from proopiomelanocortin A, recombination activating-1, rhodopsin exon 1, tyrosinase, and seven in absentia homolog 1. Primers used in polymerase chain reaction (PCR) amplification and protocols employed are those of Faivovich et al. (2005). The PCR-amplified products were cleaned with 0.5 μL of exonuclease plus 1 μL of alkaline phosphatase per 20 μL of reaction and incubated for 30 min at 37°C. Sequencing was done in both directions to check for potential errors and polymorphisms by the Macrogen Sequencing Team (Macrogen Inc., Seoul, Korea). The chromatograms obtained from the automated sequencer were read and assembled using Sequencher v5.3 (Gene Codes, Ann Arbor, MI). We performed multiple alignments using MAFFT version 7 (Katoh and Standley, 2013) with G-INS-i (global homology considered), with default parameters for gap opening and extension. The alignments were visualized in BioEdit (Hall, 1999) and concatenated using SequenceMatrix (Vaidya et al., 2011). Newly generated sequences were

deposited in GenBank under accession numbers PZ482419–PZ482426 and PZ486123–PZ486132.

Phylogenetic analysis.—Sequences of the new species were included in a reduced version of the dataset of the Hylini produced by Faivovich et al. (2018) and expanded by Chaves-Acuña et al. (2024), where we retained all samples of *Isthmohyla*, one sample per species of its closely related genera (*Hyla*, *Smilisca*, *Tlalocohyla*, and *Triprion*), and one species each of *Atlantihyla*, *Bromeliohyla*, *Charadrahyla*, *Ecnomiohyla*, *Megastomatohyla*, *Plectrohyla*, *Ptychohyla*, *Quilticohyla*, and *Rheohyla* as more distant outgroups. The trees were rooted with *Plectrohyla*. Besides the genes produced for the new species, the dataset also includes additional mitochondrial (cytochrome *b*) and nuclear gene fragments (i.e., beta-crystallin, c-myc gene exon 2, c-myc gene exon 3, prostaglandin E2 receptor EP4 subtype, protein tyrosine phosphatase non-receptor type 12, sodium/calcium exchanger 1, and tensin 3), as employed in other analyses (e.g., Faivovich et al., 2005, 2018; Wiens et al., 2005, 2010; Smith et al., 2007a, 2007b; Chaves-Acuña et al., 2024). Sequences of 28S RNA, although employed previously for the Hylini, were not included as they are not available for any species of *Isthmohyla*.

We conducted a maximum parsimony phylogenetic analysis using the software TNT v1.6 (Goloboff and Morales, 2023). Searches were done using the command "New Technology Search" under search level 15, which combines Ratchet, Tree Drifting, Sectorial Searches, and Tree Fusing (Goloboff, 1999; Nixon, 1999). For this driven search, we used the default options for these algorithms, hitting the most parsimonious trees 1,000 times. The resulting trees were submitted to a round of TBR branch swapping. Searches were done under the collapsing option "minimum length," which collapses every node whose minimum length is 0. Parsimony jackknife absolute frequencies (Farris et al., 1996) were calculated in TNT v1.6 using new technology requesting three hits with driven searches under search level 15, for a total of 1,000 replicates. Gaps were treated as fifth state, but for comparative purposes with the maximum likelihood analysis (see below), we also performed the analyses with gaps treated as missing data. For the graphic tree edition, we used the TNT script forfai.run available at https://www.lillo.org.ar/phylogeny/tnt/scripts/forfai.run, which takes as input the most parsimonious trees and the trees resulting from the resample pseudoreplicates, and outputs a strict consensus with branch lengths and support values in Newick format.

Additionally, we performed a maximum likelihood analysis with IQ-TREE v1.6.12 (Nguyen et al., 2015). Models for each molecular partition were selected using ModelFinder (Kalyaanamoorthy et al., 2017). The maximum likelihood analysis was conducted with 1,000 ultrafast bootstrap replicates (Minh et al., 2013; Hoang et al., 2018) using the option -bnni which reduces the risk of overestimating branch supports caused by severe model violations. The resulting tree (from the best scoring run with the highest log-likelihood value) was visualized and edited in FigTree 1.4.3 (Rambaut, 2014).

Isthmohyla nacientes, new species

urn:lsid:zoobank.org:act:6697571A-AB4B-4980-9908-265E1EDC167A

Hyla tica: Savage and Heyer, 1969 (part., species account); Duellman, 1970, 2001 (part., species account); Savage, 2002 (part., species account).

Isthmohyla tica: Faivovich et al., 2005 (part., first combination with *Isthmohyla*); Faivovich et al., 2018 (part., phylogenetic analysis); Hidalgo-Mora et al., 2022 (variation in adult morphology and vocalizations).

Holotype.—UCR 24345, adult male, collected from a small stream at Distrito San Lorenzo, Cantón Tarrazú, Provincia San José, Costa Rica, 9°37′15.105″N, 84°1′14.074″W, 1,455 masl, W. Chaves-Acuña, J. Abarca, A. Valverde-Castillo, J. Navarro-Picado, and M. Ureña-Chaves, 30 September 2023 (Figs. 1–3A).

Paratypes.—Nine adults collected in four localities at the Los Santos region, Provincia San José, Costa Rica (Figs. 3–4). All specimens are males unless otherwise stated: ECBAnf 50-04-0202, on a stream 1.2 km N from the type locality, in Distrito San Lorenzo, 9°37′55.412″N, 84°1′18.012″W, 1,500 masl, J. Abarca, E. Hidalgo-Mora, and J. Navarro-Picado, 29 September 2021; UCR 23769–23770, on a stream 1.2 km NW from the type locality, 9°37′37.68″N, 84°1′49.63″W, 1,455 masl, W. Chaves-Acuña, J. Abarca, and E. Hidalgo-Mora, 15 July 2022; UCR 24342–44, 24346, collected with the holotype; UCR 24367, 24368 (gravid female), at a stream 5.5 km SE from the type locality at Distrito Santa María, Cantón Dota, 9°35′29.02″N, 83°58′45.08″W, 1,400 masl, W. Chaves-Acuña, G. Chaves, T. Calleja, G. Ramírez, R. Parra, and G. Ureña, 30 October 2023.

Diagnosis.—*Isthmohyla nacientes* is a member of the *I. tica* group based on molecular evidence and some larval character states that among *Isthmohyla*—and among the Hylini—occur only in species of this group, including an enlarged oral disc that is nearly as wide as the body, multiple rows of submarginal papillae in the anterior and posterior labia, and an M-shaped anterior jaw sheath (Faivovich et al., 2018; Chaves-Acuña et al., 2025).

The new species can be diagnosed by the following characters: (1) SVL in males 34.1–37.9 mm; (2) snout rounded in dorsal view; (3) snout length 31–40% of head length; (4) tympanum with distinct annulus and membrane; (5) vocal sac bilobate; (6) vocal sac translucent; (7) nuptial pad extending from the proximal margin of the inner metacarpal tubercle to the level of the subarticular tubercle; (8) nuptial pads with rounded epidermal projections; (9) hands webbed; (10) dorsal skin with rounded or conical tubercles; (11) dorsum without distinct dorsolateral lines; (12) upper lip with dark longitudinal bars; (13) flanks with dark blotches or spots; (14) venter white with dark lateral reticulation; (15) anterior and posterior surfaces of thighs and inner edges of shanks and tarsi bright yellow-orange; (16) thighs with 4–5 transverse bars, shanks and tarsi with 5–6 each; advertisement call: (17) single note; (18) tonal; (19) note duration 10–50 ms; (20) dominant frequency 4,048–4,909 Hz; larval morphology: (21) depressed body; (22) sloping snout; (23) thick, protruded nasal rim; (24) spiracle with its opening located on the posterior third of the body and with the inner wall completely free from body; (25) oral disc width 78–82% of maximum body width; (26) deep angular folds; (27) M-shaped upper jaw sheath; (28) complete marginal papillae; (29) upper labium with 2–3 rows of submarginal papillae; (30) lower labium with 4–6 rows of submarginal papillae; (31) angular region without submarginal papillae; (32) LTRF 2/3.

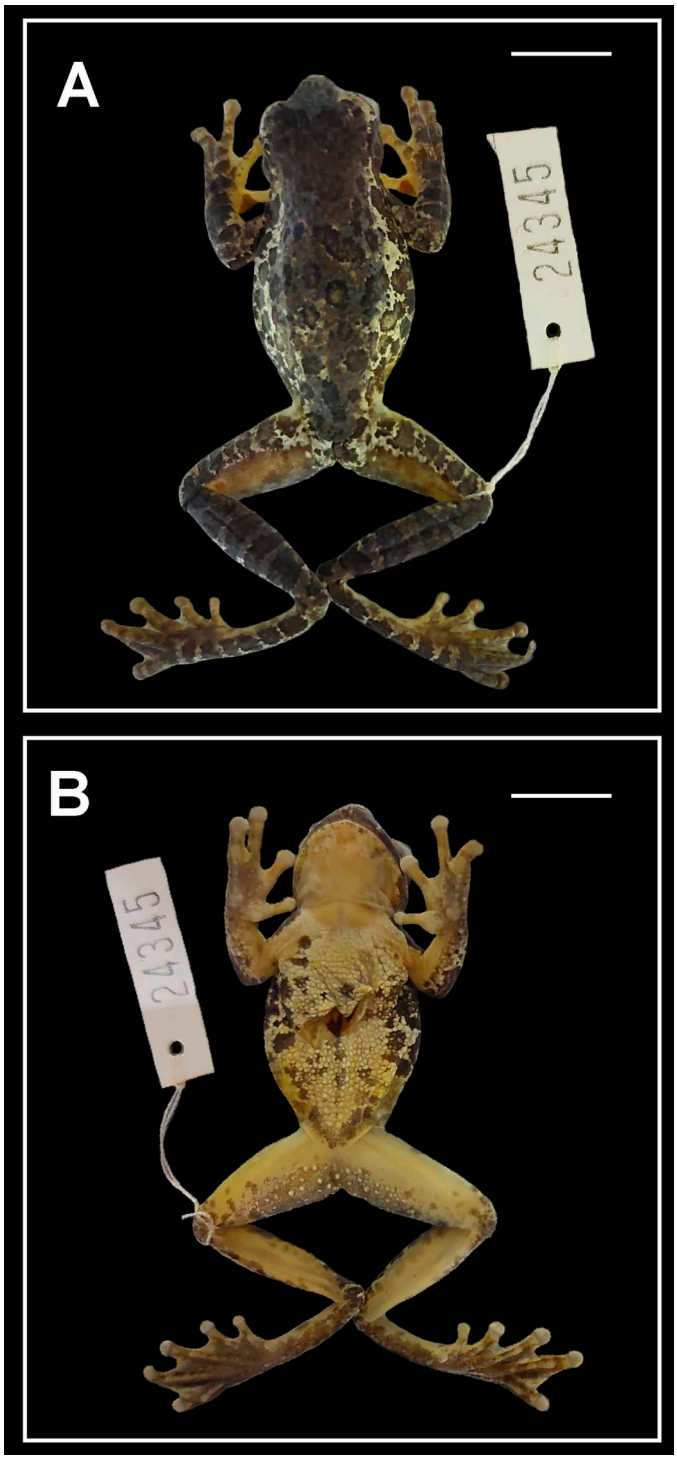

Fig. 1. *Isthmohyla nacientes*, holotype (UCR 24345; SVL 36.8 mm). (A) Dorsal view. (B) Ventral view. Scale bars = 5 mm.

***Comparison with other species of the* Isthmohyla tica *group.*—** The bilobate vocal sac distinguishes the new species from *Isthmohyla angustilineata*, *I. calypsa*, *I. graceae*, *I. lancasteri*, *I. pictipes*, and *I. rivularis* (single, subgular). The dorsum with rounded or conical tubercles distinguishes *I. nacientes* from *I. angustilineata*, *I. debilis*, *I. graceae*, and *I. xanthosticta* (smooth skin), and from *I. calypsa* (spine-shaped tubercles). The male SVL (34.1–37.9 mm) distinguishes *I. nacientes* from *I. calypsa* (27.1–28.7 mm), *I. debilis* (25–29.5 mm), and *I. lancasteri* (26–31.5 mm). A snout length 31–40% head length distinguishes *I. nacientes* from *I. calypsa* (22–25%) and *I. lancasteri* (16–23%). The rounded snout in dorsal view distinguishes *I. nacientes* from *I. calypsa*, *I. lancasteri*, and *I. xanthosticta* (truncate). The extension of the nuptial pads from the proximal margin of the inner metacarpal tubercle to the base of the subarticular tubercle distinguishes *I. nacientes* from *I. angustilineata* and *I. graceae* (extending to the base of the disc). Nuptial pads with irregular papillary epidermal projections distinguish *I. nacientes* from *I. calypsa* (spine-shaped). The tympanum with a clearly visible annulus and membrane distinguishes *I. nacientes* from *I. rivularis* (annulus partially visible under the skin). The presence of webbing on the hands differentiates *I. nacientes* from *I. angustilineata* (no webbing).

The translucent vocal sac distinguishes *Isthmohyla nacientes* from *I. angustilineata*, *I. graceae*, and *I. rivularis* (cream, dull yellow or white; with dark spots in *I. angustilineata* and *I. rivularis*), *I. calypsa* and *I. lancasteri* (white, with or without dark blotches), and *I. pictipes* (yellow, cream, or black with irregular dark blotches). The presence of dark longitudinal bars on the upper lip distinguishes *I. nacientes* from *I. angustilineata*, *I. debilis*, *I. graceae*, *I. pictipes*, *I. rivularis*, and *I. xanthosticta* (absent). The white venter with dark lateral reticulation distinguishes *I. nacientes* from *I. angustilineata*, *I. debilis*, *I. graceae*, *I. rivularis*, and *I. xanthosticta* (cream, dull yellow or white; with dark spots in *I. angustilineata* and *I. rivularis*; immaculate in *I. debilis*, *I. graceae*, and *I. xanthosticta*), *I. calypsa* and *I. lancasteri* (white with dark spots and blotches), and *I. pictipes* (dark or light background with a contrasting pattern of blotches or reticulations). The 4–5 dark transverse bars on the thighs and 5–6 bars on the shanks and tarsi distinguish *I. nacientes* from *I. angustilineata*, *I. debilis*, *I. graceae*, *I. pictipes*, *I. rivularis*, and *I. xanthosticta* (no bars), *I. calypsa* (two bars on the shanks), and *I. lancasteri* (three bars on the thighs, shanks, and tarsi). The bright yellow-orange coloration on the anterior and posterior surfaces of the thighs and the inner edges of the shanks and tarsi distinguishes *I. nacientes* from *I. angustilineata*, *I. graceae*, and *I. rivularis* (dull yellow, cream, or orange; with dark spots in *I. angustilineata* and *I. rivularis*; immaculate in *I. graceae*), *I. calypsa* and *I. lancasteri* (unpigmented, with white marks and dark blotches or spots; bright yellow with black bars in some populations of *I. lancasteri*), and *I. pictipes* and *I. xanthosticta* (brown with yellow or white spots or blotches). The flanks with dark blotches or spots distinguish *I. nacientes* from *I. angustilineata*, *I. graceae*, and *I. rivularis* (no markings), *I. debilis* (medially demarcated by a light-colored line), and *I. pictipes*, *I. tica*, and *I. xanthosticta* (with light blotches or spots). The absence of pale dorsolateral stripes on the dorsum distinguishes *I. nacientes* from *I. angustilineata* and *I. graceae* (present).

The characteristic larval morphology of the new species, with a depressed body, sloping snout, thick nasal rim, spiracle with its opening located on the posterior third of the body and with the inner wall completely free from body, an enlarged oral disc that is nearly as wide as the body, with deep angular folds, angular region devoid of submarginal papillae, multiple rows of submarginal papillae on both labia, an M-shaped upper jaw sheath and LTRF 2/3, differentiates it from *Isthmohyla angustilineata*, *I. calypsa*, *I. graceae*, and *I. lancasteri* (globular body with a rounded snout; a thin nasal rim; a spiracle with its opening located on the middle third of the body and with the inner wall fused to the body;

and a small oral disc with its width about half or less of BW, angular folds absent, angular region with submarginal papillae; arch-shaped upper jaw sheath and A-2 incomplete). Also, the labia with complete marginal papillae further differentiate the new species from *I. angustilineata* and *I. graceae* (with upper gap).

The new species is more similar to *Isthmohyla tica*, from which it differs in color pattern (see comparison above). It also differs in its advertisement call, which comprises a single, tonal note with a duration of 10–50 ms, whereas in *I. tica* the advertisement call is composed of 2–3 pulsed notes, with a duration 270–470 ms (see below).

Description of the holotype.—Body moderately robust (Fig. 1A–B); head wider than long; head as wide as the body; head length 26% SVL; head width 31% SVL. Snout rounded in dorsal and lateral view (Fig. 2A–B). Nostrils lateral, elliptical, slightly protruded; distance between nostrils 70% of IOD. *Canthus rostralis* evident and slightly concave. Loreal region slightly concave. Eyes protuberant, with ED 12% larger than IOD, surpassing END. Tympanum with distinct annuli and membrane. Tympanum rounded, separated from eye by a distance equal to TD. TD 65% of ED. Supratympanic fold evident, from the posterior corner of eye to shoulder. Vocal sac bilobate, externally evident by the loose skin on the sides of the jaw, not reaching the pectoral region (Fig. 2C).

Vomerine teeth in two arched and barely separated series, each bearing six (left) and five (right) teeth, between choanae. Choanae small, slightly quadrangular, its largest diameter less than half the length of vomerine teeth series. Tongue ovoid, free laterally and shallowly notched posteriorly. Vocal slits longitudinal, on the sides of tongue, reaching corners of the mouth.

Upper arm and forearm moderately robust. Ulnar fold poorly developed and slightly crenulated, extending from the elbow through the ventrolateral edge of the forearm and finger IV. Wrist fold evident. Fingers thick, and bearing elliptical discs, wider than long; disc on finger II smaller than the others; width of disc on finger IV about the same size of tympanum diameter (TD/3FD = 1.03). Relative finger length II < III < V < IV. Fingers with wide dermal fringes, basally webbed; webbing formula II 2–3^{-} III 2–3^{+} IV 3–2^{+} V (Fig. 2D). Outer metacarpal tubercle tripartite (Fig. 2D); inner metacarpal tubercle single, small, elliptical. Subarticular tubercles bifid; supernumerary tubercles single, rounded; conspicuous, especially on the proximal segment of finger V; in finger II, supernumerary tubercles are arranged in two rows. Dark nuptial pad, with irregular papillary epidermal projections (Fig. 2E). The pad covers dorsomedially metacarpal II and prepollex, masking the outer margin of the finger to the level of the subarticular tubercle (Fig. 2E).

Hind limbs moderately robust; TL 55% of SVL; FL 47% of SVL. Crenulated dermal fold on heel. Toes thick, with wide dermal fringes, bearing elliptical discs, wider than long. Relative toe length I< II< III< V< IV; webbing formula I 1^{+}–2^{+} II 1^{+}–2^{+} III 1^{+}–2^{-} IV 2$^{1/2}$–1$^{1/2}$V (Fig. 2F). Inner metatarsal tubercle single, oval; outer metatarsal tubercle single, rounded. Subarticular tubercles single, rounded; supernumerary tubercles single, rounded. Fringe on lateral margin of Toe V continued along the margin of the sole by a poorly developed ridge that reaches the base of the metatarsal.

The cloacal opening is directed posteroventrally near the mid-level of the thighs; it is surrounded by moderately large tubercles. Skin granular on abdomen and flanks; granular to tubercular on the upper surface of the limbs, lateral margin of forearms and tarsi, subcloacal region, and heels; shagreened to granular on dorsum of head, trunk, and limbs; smooth on throat, groin, and hidden parts of limbs.

Color in life of the holotype.—Dorsum of head, body, and limbs yellow, brown, or green, mottled throughout with green metallic flecks, and with distinct, dark-colored blotches (Fig. 3A); loreal region greenish-brown or brown, with green metallic flecks; upper lip with irregular dark longitudinal blotches separated by light patches along the lips, and an additional light spot on the tip of the snout; part of the loreal region unspotted and matching the color of the dorsum; brown canthal stripe present in some individuals; pale suborbital spot present in some individuals; iris copper-colored with fine dark reticulations; supraorbital stripe cream or light brown; tympanum darkened or brown; flanks white with dark irregular blotches scattered from the groin to the axilla (Fig. 3A); limbs, both forelimbs and hind limbs, colored similarly to the body, with dark transverse bands contrasting with the background color on both limbs; hind limbs bordered by 4–5 (thigh), 5–6 (tibia), and 5–6 (tarsus) dark transverse bars (Fig. 3B); venter white with dark lateral reticulations (Fig. 3C); gular region translucent on males (Fig. 3D), white on females; webbing on feet, hands, and axilla, as well as the anterior and posterior surfaces of the thighs, and inner edges of the tibiae and tarsi uniformly yellow-orange; groin with a bright yellow spot; edge of the forearm, heel, and cloacal opening with white or yellowish lines and/or tubercles; ventral surface of the thighs and tibiae unpigmented or partially pigmented with diffuse yellow-orange; ventral surface of the hands and feet darkened. In females, the venter is immaculate white; the yellow spot in the groin is large. By day, the orange pigment on the limbs became dull, and the green and brownish pigment on the dorsum became yellowish, with evident metallic green flecks on the background. Transversal bands on the limbs also became yellowish.

Color in preservative of the holotype.—Dorsum grayish brown marked with distinct, dark-colored blotches (Fig. 1). Green flecks on the dorsum transition to a more subdued grayish hue. Flanks appear white, and have distinct, dark-colored blotches. The venter is dull creamy white with a dark suffusion laterally.

Measurements of the holotype (mm).—SVL 36.8; HL 8.6; HW 10.1; IND 3.9; IOD 3.1; ED 3.1; END 2.1; SL 3.2; TD 1.9; FAL 6.3; TL 18.5; THL 15.4; 4FD 1.9; FL 14.9; 4TD 1.8.

Variation among paratypes.—Some measurements are included in Table 1. Vomerine teeth number varies between 4–6 (right vomer) and 5–6 (left vomer). UCR 24344, 24346, and 24367–8 have a truncate snout in profile. Three specimens (UCR 23769, 24343–4) have a straight canthus rostralis. Ulnar or tarsal tubercles protuberant (UCR 23769) or barely evident (UCR 23770, 24343–5). Dermal fold on heel not crenulated in UCR 24344, 24346, and 23769–70. In three specimens (UCR 23769, 24344, and 24346), the nuptial pad although colored, is lighter than in the holotype (see Supplemental Fig. 1A; see Data Accessibility). Outer metacarpal tubercle is tetrapartite in UCR 23769 and 23770.

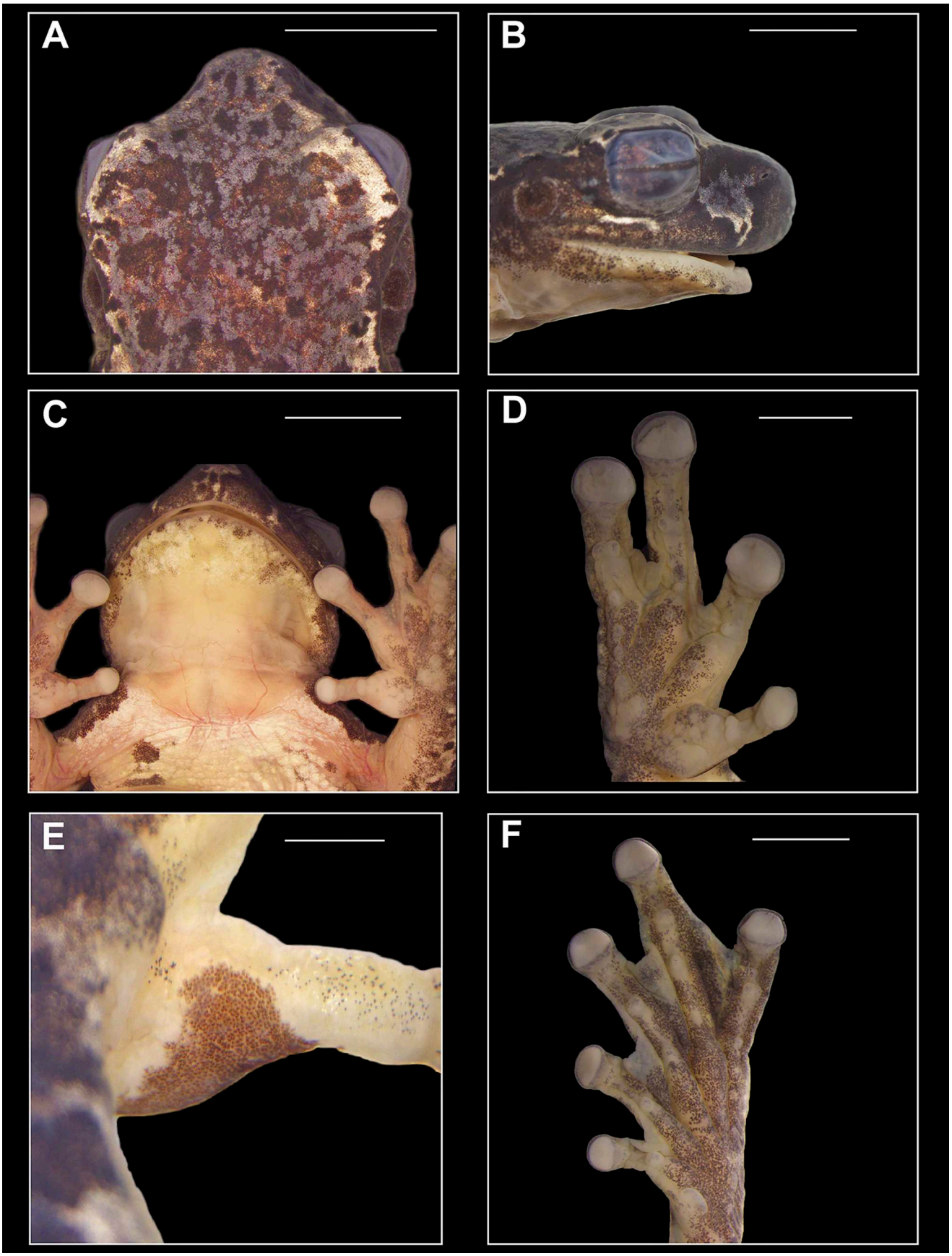

Fig. 2. *Isthmohyla nacientes*, holotype (UCR 24345). (A) Head in dorsal view. (B) Head in profile. (C) Head in ventral view. Note the bilobate, translucent vocal sac. (D) Right hand in palmar view. (E) Nuptial pad with dark colored irregular papillary epidermal projections. (F) Right foot in plantar view. Scale bars: A–C = 5 mm; D, F = 2.5 mm; E = 1 mm.

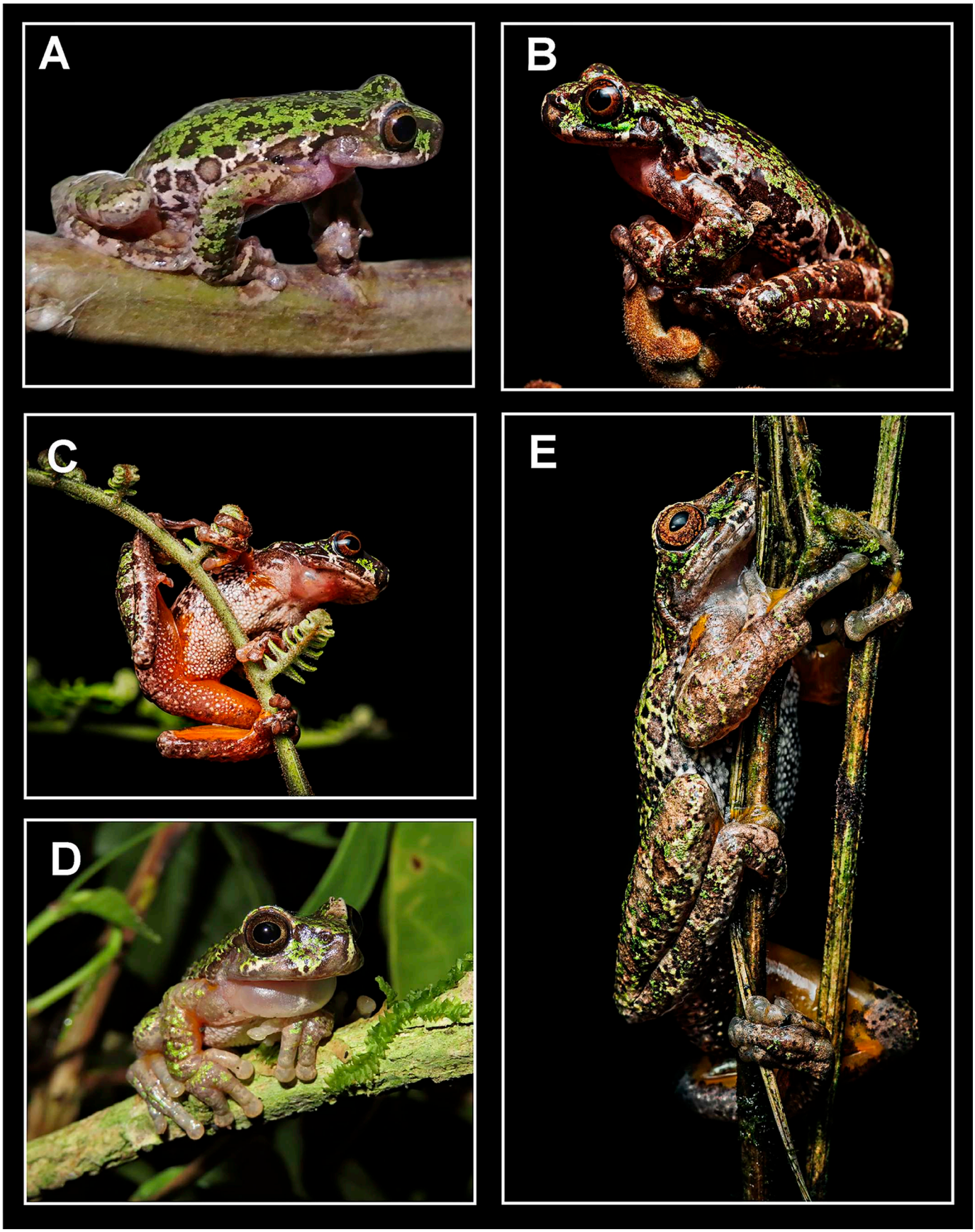

Fig. 3. *Isthmohyla nacientes* in life. (A) Holotype (UCR 24345), dorsal coloration at night. (B) Lateral view of male paratype (UCR 24367). (C) Ventral view of male paratype (UCR 24367), showing orange coloration on the hidden and ventral surfaces of the thighs and shank. (D) Male paratype (UCR 23770) showing bilobate, translucent vocal sac. (E) Lateral view of female paratype (UCR 24368). Photo credits: B, C, and E by Gabriel Ureña.

Table 1. Measurements (in mm) of the type series of *Isthmohyla nacientes*. See Materials and Methods for abbreviations.

	Males (n = 9)	Female (n = 1)
Measurements	Mean ± SD (range)	
SVL	35.8 ± 1.2 (34.1–37.8)	41.7
HL	9.3 ± 0.5 (8.5–10.2)	8.3
HW	10.6 ± 0.7 (9.7–12)	11.2
ED	2.8 ± 0.2 (2.5–3)	2.9
END	2.1 ± 0.2 (1.8–2.4)	1.9
SL	3.3 ± 0.4 (2.7–3.9)	2.7
TD	1.9 ± 0.1 (1.7–2.1)	1.9
IND	3.7 ± 0.4 (3.1–4.3)	3.1
IOD	3.2 ± 0.6 (2.3–4)	3.8
FAL	6.6 ± 0.3 (6–7.1)	6.7
TL	15.9 ± 0.7 (15.2–16.9)	17.2
THL	18.6 ± 0.4 (18.1–19.2)	19.7
FL	15.5 ± 0.9 (14.9–17.4)	17.3
4FD	1.9 ± 0.2 (1.7–2.1)	2.1
4TD	1.9 ± 0.2 (1.6–2.4)	1.4

Overall skin texture like the holotype, with some variation concerning the size and density of dorsal tubercles, which are more (e.g., UCR 23769) or less (e.g., UCR 23770, 24343) protuberant in some specimens. The number and size of the dark-colored blotches vary between individuals. Five specimens (UCR 23769–70, 24343–4, 24346) have a transversal band in the interorbital region. Some specimens (e.g., UCR 23769–70, 24346) have distinct, irregular, linear scars in the dorsum (see Supplemental Fig. 1A; see Data Accessibility), whose origin is unknown.

In life, dorsal color of head, body, and limbs yellowish or greenish brown to dark brown; in some specimens, the orbit is bordered by a thin creamy-colored line, which in some cases diffusely extends laterally onto midbody; lips greenish-brown, with tan or yellowish-tan longitudinal bars in the loreal region in some specimens (e.g., UCR 23769–70, 24346); loreal region greenish or yellowish brown; blotches on dorsum and flanks brownish or darkened; white flanks, adorned with distinct, bright yellow or orange blotches in the groin and axilla of some specimens; arms, limbs, webbing of hands and feet, and posterior surface of thighs uniformly orange or bright yellow (Fig. 3; see also Supplemental Fig. 1B–C; see Data Accessibility). Venter white suffused with different degrees of dark reticulation laterally; there are 4–6 dark-colored transversal bars each on thigh, tibia, and feet. By day, the green and brownish on the dorsum may become tan or yellowish, with evident metallic green flecks on the background or not. Transversal bands on the limbs may become yellowish or greenish.

The only available female is larger than the males (SVL 41.7 mm; see Table 1; Figs. 3E, 4). Snout is truncate in dorsal and lateral view (Fig. 4A). This specimen is more tuberculate than the available males, with prominent tarsal tubercles, and have larger bright yellow blotches in the groin and axilla (Fig. 4B–D). The subgular region is colored as the venter (Fig. 4D).

Etymology.—The specific epithet "nacientes" refers to the crucial role of headwaters and springs (*nacientes* in Spanish) in the habitat and life cycle of the new species and its stream-breeding congeners. This name highlights the species' association with aquatic environments, particularly the springs found in its range, acknowledging the ecological significance of these water sources.

Vocalizations.—Hidalgo-Mora et al. (2022) initially described the advertisement call of the new species based on three uncollected specimens, using a digital camera for recording. They characterized the vocalization as a call group consisting of non-modulated, single pulsed notes with a dominant frequency of 4,600–4,800 Hz (n = 8 call series) and a duration of 33–60 ms (n = 40 calls). These authors also described a second call type, which they referred to as a distress call, emitted during handling. The call was characterized as a non-modulated, single pulsed note with a dominant frequency of 1,839–1,862 Hz (n = 2 calls) and a duration of 10–30 ms (n = 9 calls). Expanding upon these descriptions, we present an additional analysis of the vocalizations, based on 1,161 calls from six individuals (UCR 23769–70, 24344–24346, and 24367). The recordings, totaling 83 min were conducted at an air temperature between 18–23°C, air humidity percentage of 88–93%, and water temperature of 25°C (for subaquatic calls).

We identified five different calls in *Isthmohyla nacientes*, which we refer to as calls A, B, C, D, and E. To describe call A (= advertisement call in Hidalgo-Mora et al., 2022), we examined six recordings with a total of 45 min and 607 calls obtained from four males (UCR 23769–70, 24346, and 24367; audio recordings FNJV 124945, 0124950–2, 124955–6) in their natural habitat. For calls B, C, and D, we recorded one male in captive conditions (UCR 24367), which vocalized in a courting context when in close proximity to a gravid female (UCR 24368). For call B, we examined two recordings with a total of 8 min and 361 calls (audio recordings FNJV 124946, 124949). For call C, we examined two recordings with a total of 10 min and 128 calls (audio recordings FNJV 124947, 124949). For call D, we examined one recording with a total of 10 min and 27 calls (audio recording FNJV 124948). For call E (= distress call in Hidalgo-Mora et al., 2022), we examined two recordings with a total of 10 min and 38 calls from two individuals in captivity (UCR 24344–5; audio recordings FNJV 124953–4). See Table 2 for values of spectral and temporal parameters of the calling repertoire of *I. nacientes*.

Call A (Fig. 5A–D) corresponds to the advertisement call of *Isthmohyla nacientes*, composed of a single high-frequency, modulated, pulsatile note, which is emitted singly or within a call series (Fig. 5A–B). The call is amplitude modulated with the peak occurring at the beginning or middle of the call, which lasts 10–50 ms (Fig. 5C–D). When emitted in series, it can contain up to 625 notes and last up to 151 s. Intercall intervals vary from 100 to 300 ms, and call repetition rate varies from 4.1 to 4.8 calls/s. The minimum frequency is 3,962–4,737 Hz and the maximum frequency 4,134–4,995 Hz. The dominant frequency is 4,048–4,909 Hz. Calls typically exhibit ascending frequency modulation.

Call B (Fig. 5E–H) is composed of a single high-frequency, pulsatile note, only registered within a call series under a courtship event (Fig. 5E–F). The call is amplitude modulated with the peak occurring at the beginning or middle of the call, which lasts 30–210 ms (Fig. 5G–H). Call series can contain up to 361 notes emitted in 45 s, with intercall interval ranging from 10–100 ms and note repetition rate of about 8

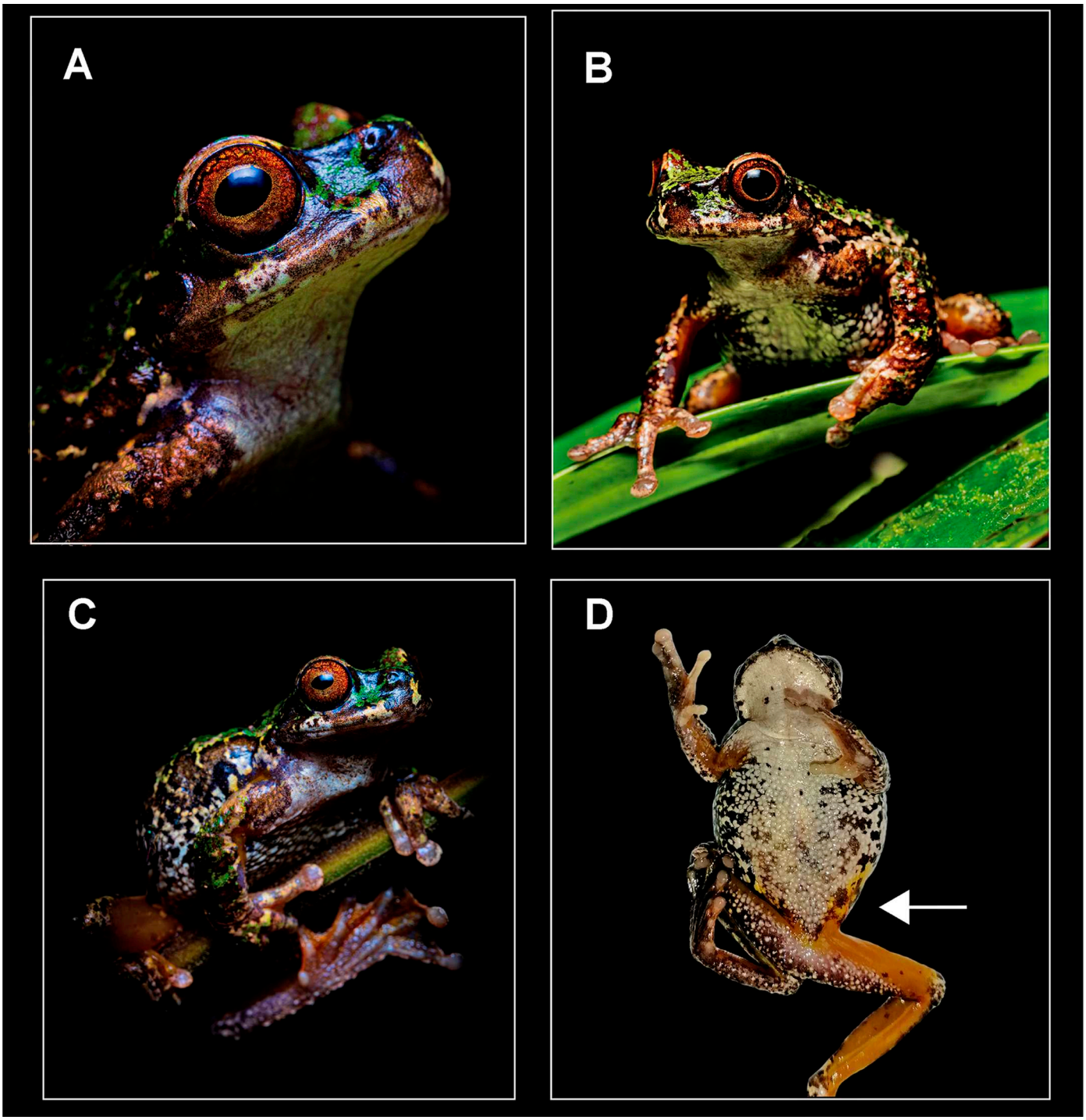

Fig. 4. *Isthmohyla nacientes*, female paratype (UCR 24368). (A) Detail of snout in profile. (B) Anterior view, note conspicuous tubercles on the dorsum and arms. (C) Lateral view. (D) Ventral view. The solid arrow points to the bright yellow blotch in the groin. Photo credits: A and C by Gabriel Ramírez; B by Gabriel Ureña.

calls/s. The minimum frequency is 3,789–4,478 Hz and the maximum frequency 4,048–4,737 Hz. The dominant frequency ranged from 4,134 to 4,220 Hz. Call B exhibits no frequency modulation.

Call C (Fig. 6A–D) was emitted on land and underwater when the male pursued the female during the courtship event (Fig. 6A–B). It consists of a low frequency, pulsatile call, which is amplitude modulated with the peak occurring at the beginning or end of the call duration, which lasts 10–20 ms (Fig. 6C–D). The minimum frequency is 1,722–3,617 Hz and the maximum frequency 2,067–4,048 Hz. The dominant frequency is 1,981–3,789 Hz. Call C exhibits an ascending frequency modulation.

Call D (Fig. 6E–H) corresponds to a second type of subaquatic courtship call. This type of call was recorded mostly underwater while both male and female were completely submerged. Before the emission of this type of call, the male was emitting calls B and C interchangeably for a long period

Table 2. Acoustic parameters of the vocalizations of *Isthmohyla nacientes* recorded at different localities of the Los Santos region, Costa Rica. Air temperature and air humidity varied between 19–23°C and 89–93%, respectively. Values are reported as mean ± SD (range). Advertisement calls are deposited in the FNJV under catalog numbers 124945, 124950–2, 124955–6; courtship calls are archived under FNJV 124946–9; release calls are archived under FNJV 124953–4.

Call parameters	Call A (advertisement)	Call B (courtship)	Call C (courtship, subaquatic)	Call D (courtship, subaquatic)	Call E (release)
n	607	361	128	27	38
Note duration (ms)	30 ± 20 (10–50)	100 ± 20 (30–210)	60 ± 30 (10–20)	80 ± 50 (20–200)	20 ± 10 (10–80)
Minimum frequency (Hz)	4,421 ± 171 (3,962–4,737)	4,138 ± 97 (3,789–4,478)	2,387 ± 661 (1,722–4,306)	1,633 ± 274 (1,205–1,981)	1,969 ± 234 (1,722–2,670)
Maximum frequency (Hz)	4,635 ± 175 (4,134–4,995)	4,378 ± 114 (4,048–4,737)	2,666 ± 678 (2,067–4,565)	2,079 ± 148 (1,808–2,497)	2,243 ± 237 (1,981–3,014)
Dominant frequency (Hz)	4,528 ± 179 (4,048–4,909)	4,253 ± 102 (4,048–4,651)	2,557 ± 680 (1,981–4,392)	1,847 ± 238 (1,378–2,067)	2,119 ± 234 (1,894–2,842)
Frequency bandwidth (Hz)	210 ± 62 (86–602)	239 ± 67 (86–516)	290 ± 163 (86–947)	446 ± 234 (172–947)	274 ± 74 (172–516)
Air temperature (°C)	18–23	22	21	23	22
Air humidity (%)	88–93	90	89	88	89
Water temperature (°C)	–	–	25	25	–

of time (2 hours) as he followed the female throughout the terrarium. The female sought underwater shelter between rocks, and the male emitted the call before he tried to grab the female to accommodate the amplectic position (see details below). Call D consists of a low-frequency, modulated, tonal call, which is amplitude modulated with the peak occurring at the beginning or end of the note (Fig. 6E–H). The call duration ranges from 20–200 ms. The minimum frequency varies from 1,205–1,981 Hz, and the maximum frequency ranges from 1,808–2,497 Hz; the dominant frequency is 1,378–2,067 Hz. Call D exhibits an ascending frequency modulation toward the end of the call duration or none.

Call E (Fig. 6I–L) was emitted when frogs were being handled, presumably in the context of a release behavior. Call E is similar to call C, but the latter is longer and encompasses narrower spectral values (Fig. 6I–L). Call E consists of a low-frequency, tonal call, which is amplitude modulated with the peak occurring at the end of the note. The call duration ranges from 10–80 ms. The minimum frequency is 1,722–2,670 Hz, and the maximum frequency varies from 1,981–3,014 Hz. The dominant frequency is 1,894–2,842 Hz. Call B exhibits an ascending frequency modulation.

***Comparison with advertisement calls of other species in the* Isthmohyla tica *group.*—**The advertisement call of *Isthmohyla nacientes* is composed by a single tonal note, with a duration of 10–50 ms and a dominant frequency of 4,048–4,909 Hz. These characteristics distinguish the call of this species from that of *I. angustilineata* (pulsed call, duration 130–300 ms, dominant frequency 1,593–1,875 Hz), *I. calypsa* (pulsed call, duration 110–190 ms, dominant frequency 3,710–4,048 Hz), *I. debilis* (pulsed call, duration 61–173 ms, dominant frequency 5,167–5,857 Hz), *I. graceae* (pulsed call, dominant frequency 750–2,756 Hz), *I. lancasteri* (call composed of 1–2 pulsed notes, with two co-dominant frequencies at 1,636–2,239 Hz and 3,445–4,392 Hz), *I. pictipes* (pulsed call, duration 200–300 ms, dominant frequency 2,411–3,617 Hz), *I. rivularis* (pulsed call, dominant frequency 2,325–2,928 Hz), and *I. tica* (call composed of 2–3 pulsed notes, duration 270–470 ms; see Supplemental Fig. 2; see Data Accessibility).

To the human ear, the call of *Isthmohyla nacientes* bears a remarkable similarity with that of the dendrobatid *Silverstoneia flotator*, a leaf-litter species that produces short, tonal notes (30–50 ms), typically assembled in series within a dominant frequency of 5,100–6,300 Hz (Ibáñez and Smith, 1995). It also resembles the call of an unknown syntopic orthopteran, which emits short, tonal calls (65–69 ms), organized in series with frequencies around 3,700 Hz (WCA, pers. obs., FNJV 0124957–8).

***Tadpoles.*—**Description based on four specimens in stages 27–28 (UCR 24429) and one in stage 35 (UCR 23776). See Table 3 for individual measurements. Tadpoles belong to Guild II (exotrophic), category C (lotic only), and category 10 (adherent) as per McDiarmid and Altig's (1999) classification. Body depressed (BH/BW = 0.84–0.87), elliptical in dorsal view (Fig. 7A); in lateral view, ventral contour flat in the peribranchial region, convex in the abdominal region (Fig. 7B); 27–30% total length. Tail long, 70–73% total length. Snout rounded in dorsal view (BWN/BWE = 0.71–0.73) and sloping in profile (Fig. 7B; see also Supplemental Fig. 3A; see Data Accessibility). Eyes small (ED/BWE = 0.20–0.21), located

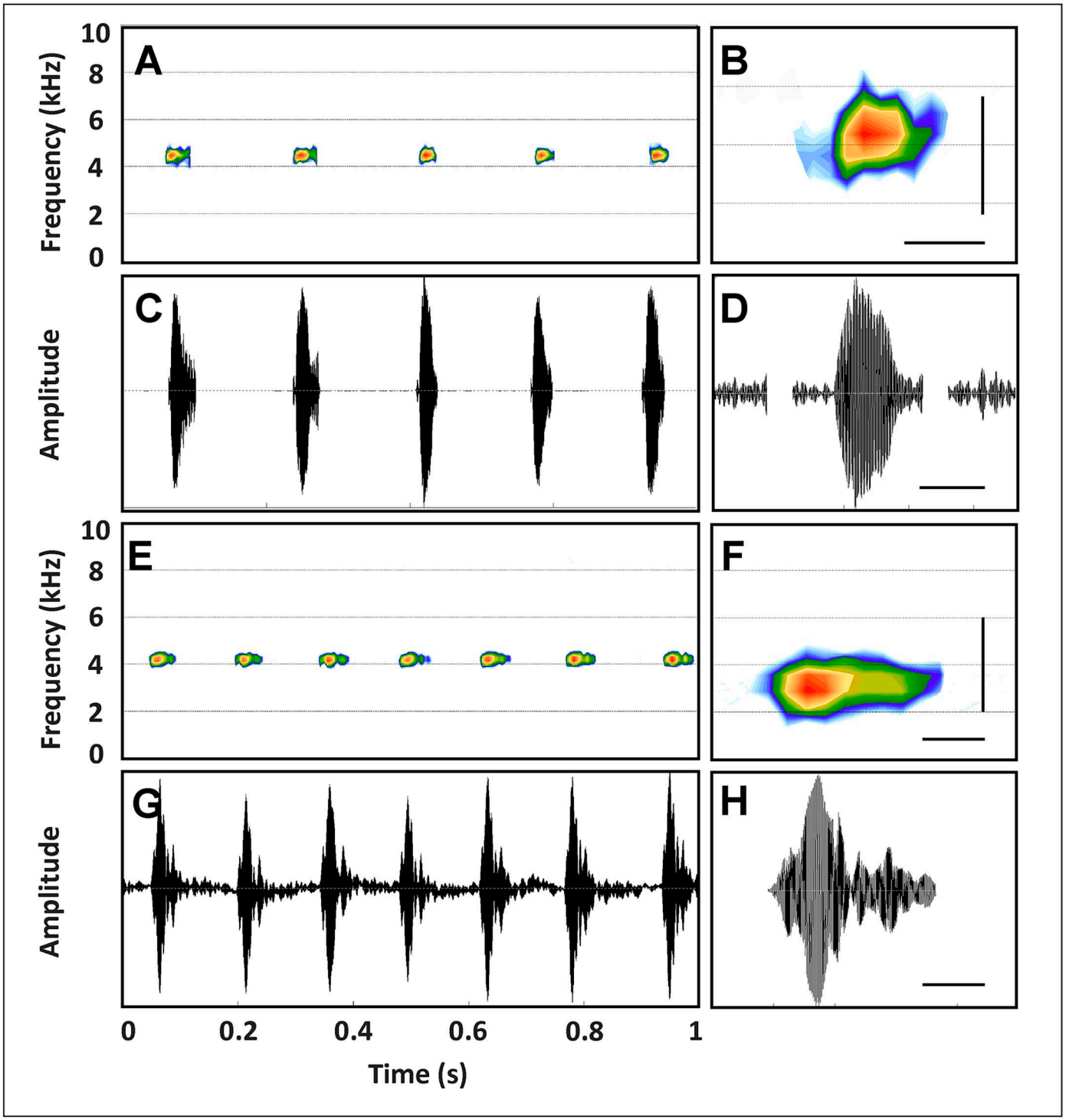

Fig. 5. Spectrograms (above) and oscillograms (below) of vocalizations of *Isthmohyla nacientes*, male paratype (UCR 24367) recorded at Santa María de Dota, San José Province, Costa Rica. (A–D) Recordings obtained from the natural habitat corresponding to call type A (recording FNJV 124945). (E–H) Recordings obtained under captivity corresponding to call type B (recording FNJV 124946). (A, B, E, F) Spectrograms. (C, D, G, H) Oscillograms. Note the difference in call rate and call duration between the two call types. Scale bar = 200 ms (horizontal), 1,000 Hz (vertical).

dorsally (IOD/BWE = 0.61–0.69), directed dorsolaterally. Nostrils rounded, small (ND/ED = 0.14–0.19), directed anterolaterally, and with a thick fleshy rim that is notably protruded; nostril–snout distance 66–68% of eye–snout distance. Spiracle sinistral, lateral (SVD/BH = 0.25–0.36), directed posteriorly, short (SL/BL = 0.07–0.10), opening at the posterior third of the body (SSD/BL = 0.80–0.89); inner wall completely free from body (Fig. 7B, D). Intestinal tube circularly coiled, switchback point located at the center of abdominal region. Vent tube dextral, directed posteriorly, laterally fused to margin of ventral fin; ventral and dorsal walls of same length.

Oral disc large (ODW/BW = 0.78–0.82), positioned ventrally (Fig. 7C, E; see also Supplemental Fig. 3B; see Data Accessibility); bordered by a complete row of single or

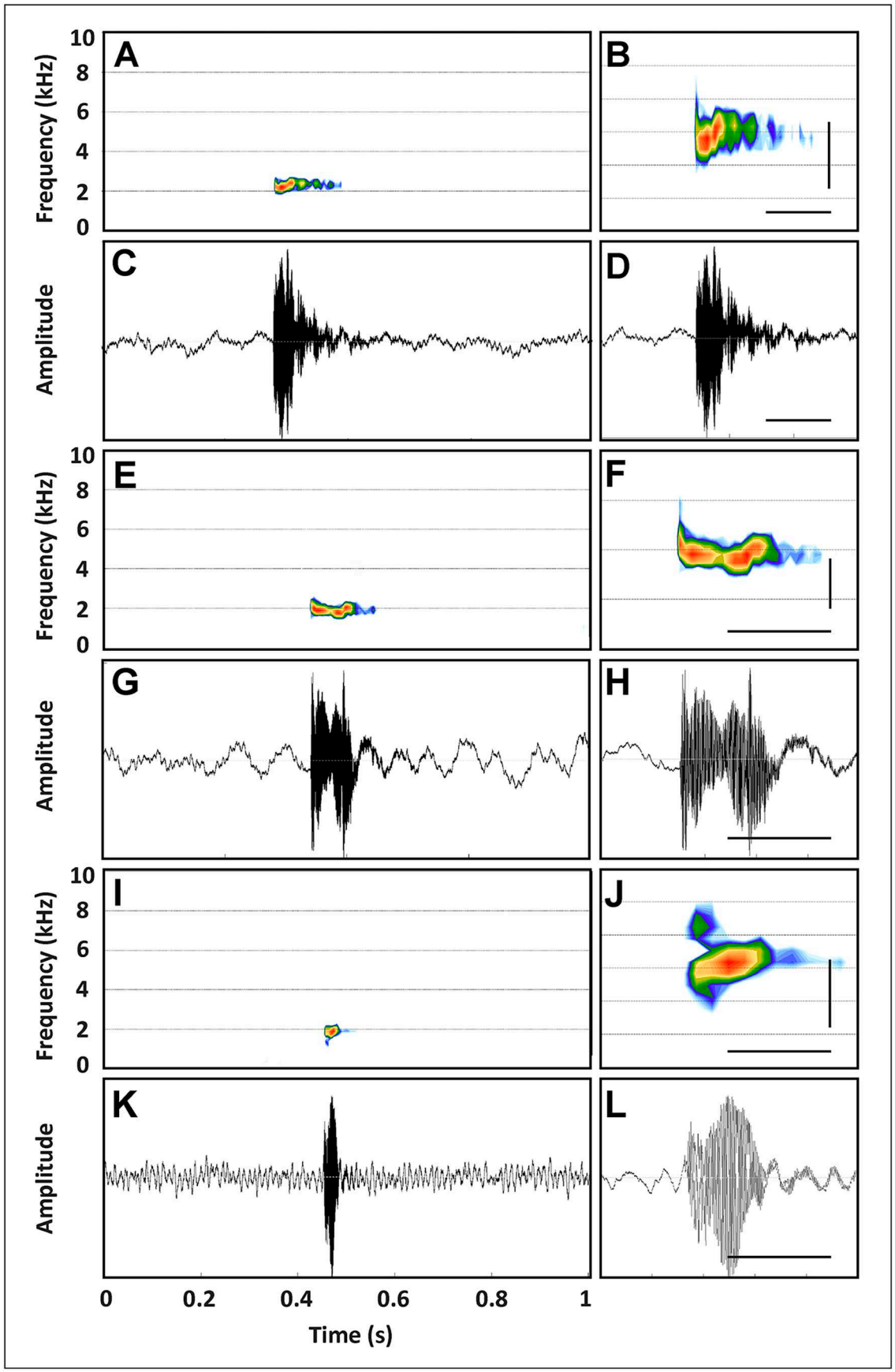

Fig. 6. Spectrograms (above) and oscillograms (below) of vocalizations of *Isthmohyla nacientes* obtained from a male paratype (UCR 24367) in captivity. (A–D) Courtship call recorded on land (recording FNJV 124947). (E–H) Courtship call recorded underwater (recording FNJV 124948). (I–L) Release call (recording FNJV 124953). Scale bar = 200 ms (horizontal), 1,000 Hz (vertical).

Table 3. Some measurements (in mm) of tadpoles of *Isthmohyla nacientes* ($n = 5$). See Materials and Methods for abbreviations.

	Tadpole stage (*n*)		
Variable	27 (1)	28 (3)	35 (1)
TL	26.6	28.8–33.1	50
BL	10	9.3–12.6	13.7
TAL	16.6	19.5–20.5	6.8
MTH	5.2	5.7–5.8	8.3
IND	2.7	2.8–3.3	4.1
IOD	3.1	3.2–4	5.7
TMH	3.2	4.2–4.4	5.7
TMW	2.9	3.4–4.1	5.9
BW	6	6.6–6.8	9.9
BWN	5.6	4.7–5.9	6.8
BWE	6	5.8–6.4	9.3
BH	5.1	5.7–5.8	8.7
END	0.6	0.9–1.5	2.2
NSD	2.7	3–3.1	4.4
ED	1.1	1.2–1.3	2
ND	0.3	0.2–0.3	0.3
SSD	7.2	6.7–9.3	11.1
ODW	5.2	5.5–5.9	7.8
DFH	1.7	1.6–1.8	2.6
VFH	1.4	1.4–1.7	2.2
SL	1	0.9	1.4
SVD	1.5	1.7	3.7

biserial marginal papillae, with a small medial emargination. Upper labium with 2–3 rows of small, conical or triangular submarginal papillae above the angular area, extending medially to the central region of the labium; the lower row continues medially as a single, continuous row of enlarged, quadrangular papillae, located above A-1. Lower labium with 2–3 rows of small, conical or triangular submarginal papillae proximal to the angular area, extending medially to the central region of the labium and expanding to form 4–6 irregular rows; the uppermost submarginal papilla row continues medially as quadrangular or conical papillae; submarginal papillae larger than marginal papillae; deep angular folds devoid of submarginal papillae in the labial margin. LTRF 2/3, all tooth rows with the same length. The labial tooth size varies, with those in the central portions of P1 > A2 ≈ A1 > P2 > P3, those toward the lateral portions smaller. Jaw sheaths narrow, finely serrated, upper jaw sheath M-shaped; lower jaw sheath with concave free margin, V-shaped; upper jaw sheath wider than lower (Fig. 7D–E; see Supplemental Fig. 3B–C; see Data Accessibility).

Caudal musculature robust (TMH/BH = 0.6–0.8), almost reaching tail tip; tail tip rounded. Dorsal fin low (DFH/TAL = 0.08), higher than ventral fin (DFH/VFH = 1.10–1.19) and originating near the base of the tail, but it is notably low on the anterior third of the tail, at which point it begins to expand, reaching its maximum height at the middle of the dorsal margin of the tail, where the free margin of the fin is convex to the longitudinal axis. Ventral fin low (VFH/TAL = 0.07), free margin slightly convex, originating at level of vent tube. Maximum height of dorsal and ventral fin at the last third of the tail.

Tadpole coloration in preservative.—Body light to dark brown, marbled with irregular rounded dark brown spots dorsally and laterally; venter is translucent with scattered melanophores in the most posterior part, near the vent tube. Tail musculature cream with few scattered rounded black spots.

Tadpole coloration in life.—Body light brown to gray, densely speckled with iridophores and irregular black spots dorsally and laterally. Venter translucent, maculated with melanophores and iridophores; spiracle translucent. Iris black, densely covered with iridophores, but exposing dark areas. Tail musculature light brown to gray with distinct, irregular, dark-colored blotches dorsally and laterally on the most anterior part; fins translucent with brown flecks (see Supplemental Fig. 4; see Data Accessibility).

Comparison with other tadpoles of the* Isthmohyla tica *group.—The tadpole of *Isthmohyla nacientes* is more similar to larvae of closely related stream-breeding species within the *I. tica* group (*I. debilis*, *I. pictipes*, *I. rivularis*, and *I. tica*). These similarities include a depressed body; sloping snout; spiracle with a free inner wall and with its opening located in the posterior third of the body; an enlarged oral disc that is nearly as wide as the body (ODW 73–88% in *I. debilis*; 78–82% in *I. nacientes*; 76–90% in *I. pictipes*; 74–92% in *I. rivularis*; 70–81% in *I. tica*); deep angular folds in the oral disc; complete row of marginal papillae; multiple rows of submarginal papillae in the upper and lower labia; M-shaped upper jaw sheath; and LTRF 2/3, with complete tooth rows (see Supplemental Fig. 3; see Data Accessibility). The absence of submarginal papillae in the angular region distinguishes the larva of the new species from that of *I. debilis* (few papillae; Chaves-Acuña et al., 2025) and *I. rivularis* (numerous papillae; see Duellman, 1970; confirmed by examined specimens).

Distribution.—*Isthmohyla nacientes* has been collected in four localities of the Los Santos region, central Pacific of Costa Rica (Fig. 8A). An additional specimen of this species (KU 91691) was collected in San Isidro del General, San José Province at 2,000 masl, 34 km SE from the easternmost locality reported in this study in the Canton Dota.

Natural history.—*Isthmohyla nacientes* has been observed in pristine environments surrounded by mature forests and undisturbed aquatic ecosystems (Fig. 8B), as well as in various altered environments along the banks of rivers (Fig. 8C). These altered environments include vegetation in early stages of plant succession, such as thickets, shrubs, pastures, herbaceous vegetation, and secondary growth forests. The new species has been found within coffee plantations and in areas polluted with solid waste near sewers or roadside bushes, where they have been observed perching in large rocks and coffee plants.

Males are commonly observed calling from vegetation or rocks up to 3 meters above water level along the stream margins. They call from several meters apart, and small aggregations, including adult males and juveniles have been observed (see Supplemental Fig. 5A–C; see Data Accessibility). Calling activity occurs during day and night. Only in calls A and B did the male expand its vocal sac. In calls C, D, and E, the male performed body side vibrations when producing the sounds. Calls C and D were emitted on land but also while both male and female were completely submerged underwater, especially call D. Females have been observed

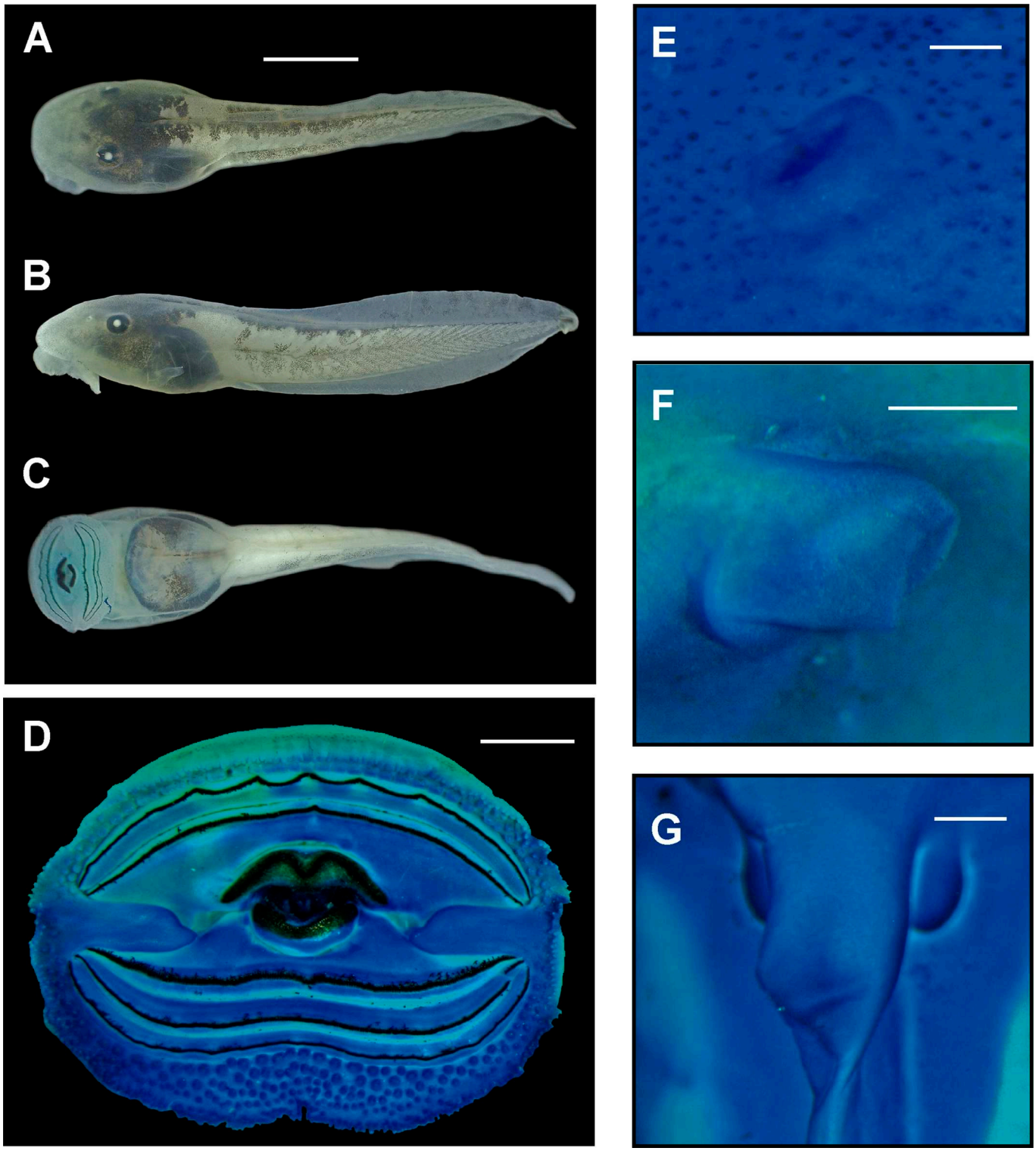

Fig. 7. *Isthmohyla nacientes*, tadpole (UCR 23766), stage 28. (A) Dorsal view. (B) Lateral view. (C) Ventral view. (D) Oral disc. (E) Nostril. (F) Spiracle. (G) Vent tube. Scale bars: A–C = 5 mm, D = 1 mm, E = 0.1 mm, F–G = 0.5 mm.

perched on leaves and branches overhanging water at heights ranging between 2 to 2.5 m. Syntopic frog species encountered at the same streams where we documented *Isthmohyla nacientes* include *Agalychnis annae*, *Craugastor crassidigitus*, *C. stejnegerianus*, *Duellmanohyla legleri*, *D. rufioculis*, *Espadarana prosoblepon*, *I. pseudopuma*, *Lithobates taylori*, *Pristimantis cruentus*, *P. ridens*, *Smilisca phaeota*, and *S. sordida*.

In captivity, the male exhibited continuous calling for around thirty hours, predominantly emitting call B at a high rate and intermittently alternating between calls B and C. Throughout this time, the male actively pursued the female, while it consistently evaded his advances by seeking refuge between rocks underwater, often remaining completely submerged. Notably, when the male increased the rate of its call, the female

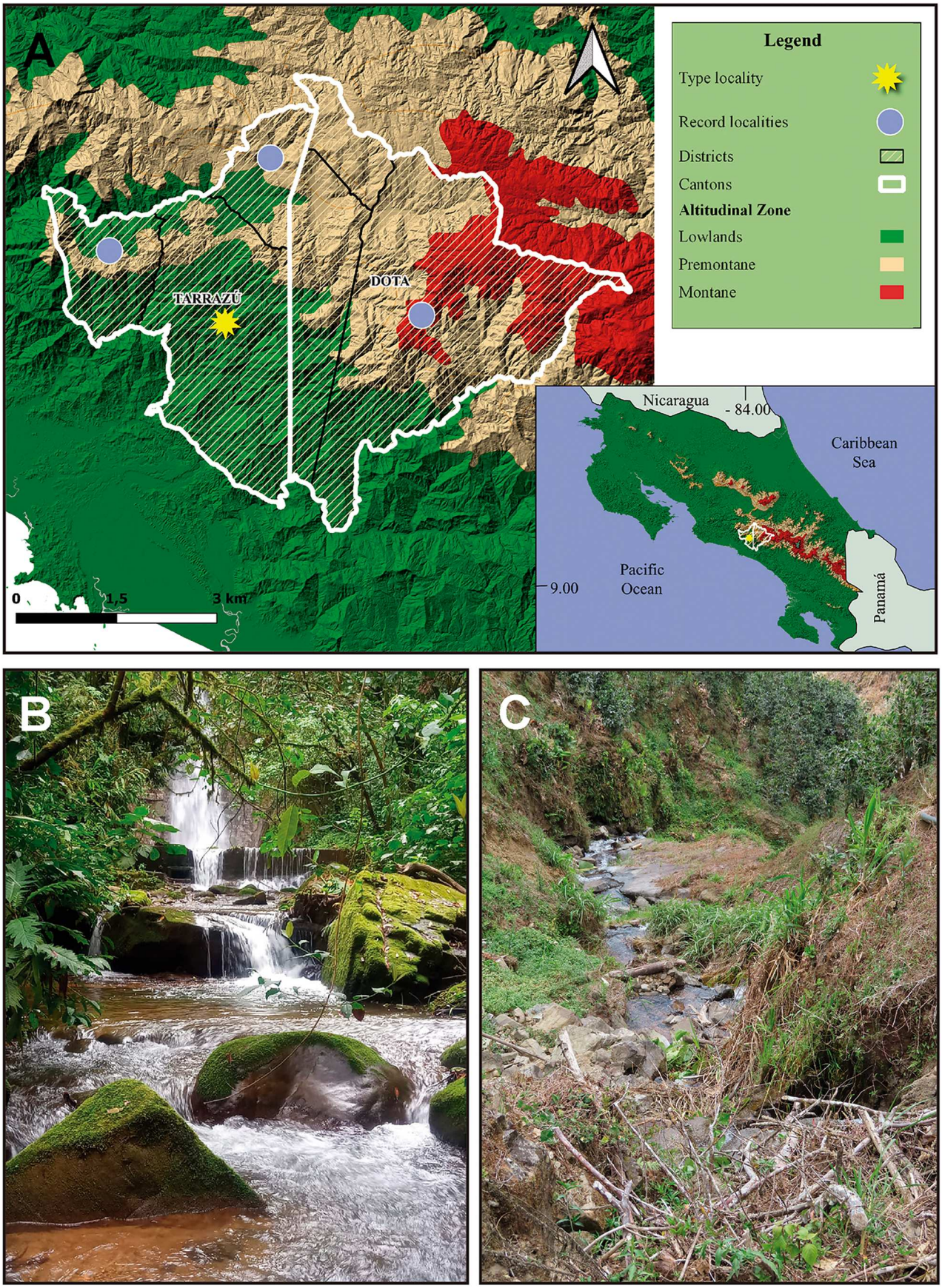

Fig. 8. Distribution of *Isthmohyla nacientes*. (A) Localities where the species is known to occur in the Los Santos region (Dota and Tarrazú cantons, San José Province, Costa Rica). (B) Pristine habitat in Dota. (C) Disturbed habitat in Tarrazú.

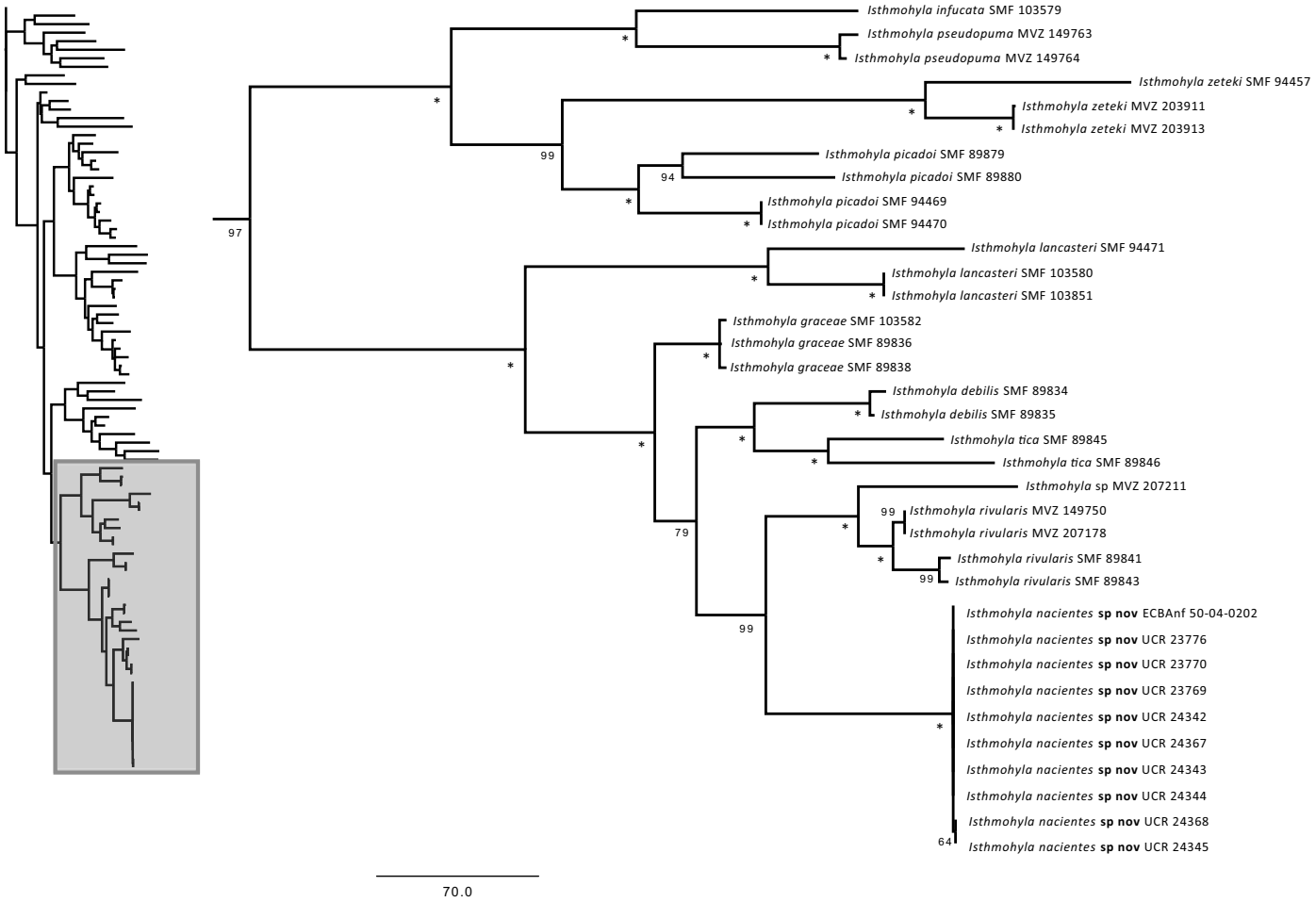

Fig. 9. Strict consensus of the 66 most parsimonious trees of the analysis using gaps as fifth state (length 17,928 steps). Portion of the tree showing the results for the genus *Isthmohyla*. The left inset shows the section of the full tree of Supplemental Fig. 6 (see Data Accessibility) that is shown here. Values around the nodes are jackknife absolute frequencies. Nodes lacking values have frequencies < 50%. An asterisk (*) indicates 100% frequency.

displayed an apparent attraction to the male. Additionally, we observed the male emitting call D underwater before attempting to grasp the female while both were completely submerged. Despite these behaviors, the pair was never observed in amplexus. Following the male's cessation of calling after this event, it did not resume calling in the subsequent days. Intriguingly, we noted that the female spent a considerable amount of time underwater, both during the courtship event and when the male was not active. Although we did not account for the time spent underwater, on one occasion, the female remained completely submerged for several minutes. The female contained 211 ovarian unpigmented eggs with a diameter of 1.82–2.50 mm (n = 20). The amplexus, egg mass, and oviposition site are not known.

Tadpoles were active during day and night, in streams located in open habitats where sunlight can reach the stream bed. Larvae were collected at the type locality and 3.5 km W. Tadpoles are benthic and are typically found in pools along open areas and/or disturbed forest habitats. The dorsal color of the tadpoles allows them to blend in with the rocks and substrate of the streams.

Phylogenetic relationships and genetic distances.—The phylogenetic analysis with maximum parsimony considering gaps as fifth state resulted in 66 trees (17,928 steps; Fig. 9; Supplemental Fig. 6; see Data Accessibility); the results are fully congruent with those considering gaps as missing data, and the maximum likelihood tree (Supplemental Fig. 7; see Data Accessibility). *Isthmohyla nacientes* is recovered as the well-supported (94% jackknife) sister taxon of a clade including *I. rivularis* and a candidate species, *Isthmohyla* sp., from northern Costa Rica (see Faivovich et al., 2018). The uncorrected p-distances for the 16S gene fragment of *Isthmohyla* sp. and *I. rivularis* with *I. nacientes* are 4.07–4.24% and 4.24–4.76%, respectively. See Table 4 for the uncorrected p-distances between *I. nacientes* and the other species of the *I. tica* group for which sequences are available (i.e., *I. debilis*, *I. graceae*, *I. lancasteri*, and *I. tica*; Faivovich et al., 2018).

DISCUSSION

Our results corroborate the monophyly of the well-supported *Isthmohyla tica* group (jackknife 100%), as previously supported by Faivovich et al. (2018) and Chaves-Acuña et al. (2024). The species of this group that have not been included in the phylogenetic analyses are *I. angustilineata*, *I. calypsa*, *I. pictipes*, and *I. xanthosticta*. Our results in general have higher jackknife support values than those of Faivovich et al. (2018) and Chaves-Acuña et al. (2024), possibly because the dataset is much smaller than in those studies, being restricted to *Isthmohyla* and more closely related taxa. Furthermore, our results

Table 4. Uncorrected p-distances between the 16S fragment among some of the type specimens of *Isthmohyla nacientes* and the other species of the *I. tica* group, expressed as percentage. Specimens marked with an asterisk are larvae.

	1	2	3	4	5	6	7	8	9	10	11	12	13	14	15	16	17	18	19
I. nacientes ECBAnf 50-04-0202	–																		
I. nacientes UCR 23776*	0.17	–																	
I. nacientes UCR 23776*	0.17	0.00	–																
I. nacientes UCR 23770	0.17	0.00	0.00	–															
I. nacientes UCR 23769	0.17	0.00	0.00	0.00	–														
Isthmohyla sp. MVZ 207211	4.07	4.24	4.24	4.24	4.24	–													
I. rivularis MVZ 149750	4.24	4.41	4.41	4.41	4.41	3.22	–												
I. rivularis SMF 89841	4.59	4.76	4.76	4.76	4.76	3.23	1.87	–											
I. rivularis SMF 89843	4.59	4.76	4.76	4.76	4.76	3.23	1.87	0.00	–										
I. tica SMF 89845	4.08	4.25	4.25	4.25	4.25	3.74	3.74	3.74	3.74	–									
I. tica SMF 89846	5.11	5.28	5.28	5.28	5.28	3.91	3.74	3.23	3.23	1.87	–								
I. debilis SMF 89834	5.44	5.61	5.61	5.61	5.61	5.10	4.41	4.07	4.07	3.40	3.40	–							
I. debilis SMF 89835	5.61	5.78	5.78	5.78	5.78	4.93	3.91	3.74	3.74	3.23	3.23	0.51	–						
I. lancasteri SMF 94471	9.28	9.45	9.45	9.45	9.45	8.75	8.23	8.06	8.06	8.75	7.56	8.74	8.92	–					
I. lancasteri SMF 103580	9.96	10.13	10.13	10.13	10.13	9.60	8.40	8.57	8.57	8.92	8.24	9.42	9.60	3.76	–				
I. lancasteri SMF 103851	9.96	10.13	10.13	10.13	10.13	9.60	8.40	8.57	8.57	8.92	8.24	9.42	9.60	3.76	0.00	–			
I. graceae SMF 103582	3.90	4.07	4.07	4.07	4.07	3.56	3.40	3.40	2.89	3.23	3.57	3.40	7.37	8.41	8.41	0.00	–		
I. graceae SMF 89836	4.07	4.24	4.24	4.24	4.24	3.73	3.40	3.40	3.06	3.40	3.74	3.23	7.54	8.58	8.58	0.17	0.00	–	
I. graceae SMF 89838	3.90	4.07	4.07	4.07	4.07	3.56	3.40	3.40	2.89	3.23	3.57	3.40	7.37	8.41	8.41	0.00	0.17	0.00	–

corroborate the monophyly of a clade within the *I. tica* group that includes the stream-breeding species *I. debilis*, *I. nacientes*, *I. rivularis*, *I. tica*, and, tentatively, *I. pictipes*.

Our findings reveal intriguing aspects of the reproductive biology of *Isthmohyla nacientes* in terms of the observed behaviors in captivity (i.e., the female's response to increased calling rates, the prolonged time spent underwater by both male and female, the species' diverse vocal repertoire encompassing high- and low-frequency calls, and the emission of subaquatic calls by the adult male before attempting amplexus). Yet, more research is needed to better understand the broader implications of subaquatic calls in *I. nacientes*, emphasizing the importance of exploring their occurrence outside of water and their potential influence on reproductive success under natural conditions.

Our report on subaquatic calls in *Isthmohyla nacientes* parallels observations in other families such as the Pelobatidae (Lizana et al., 1994), Ranidae (Zheng, 2019), Megophryidae (Zheng et al., 2011), and Telmatobiidae (Brunetti et al., 2017). However, contrary to most underwater advertisement calls reported in these groups of typically aquatic anurans, our findings pertain to subaquatic courtship encounters of a terrestrial species commonly inhabiting vegetation overhanging streams. Within the Hylidae, the production of subaquatic calls in *I. nacientes* represents the second known instance of this behavior, with the other being *Plectrohyla avia* (Hylini; Barrio-Amorós et al., 2016).

While knowledge on reproductive biology is still quite limited for species of the *Isthmohyla tica* group (Trueb, 1968; Myers and Duellman, 1982; Lips, 1996), there are some reports based on dissected females. In this regard, differences in egg pigmentation were noted in the *I. tica* group, with unpigmented eggs observed in *I. calypsa* (Lips, 1996), *I. debilis* (Chaves-Acuña et al., 2025), *I. nacientes* (this study), *I. pictipes* (WCA, pers. obs., KU 103965), and *I. rivularis* and *I. tica* (Starrett, 1966), whereas pigmented animal poles are reported in *I. angustilineata* (WCA, pers. obs., MHCH 5057), *I. graceae* (M. Quiroz and E. Griffith, pers. comm.), and *I. lancasteri* (Lips, 1996). These occur as well in *I. pseudopuma* (Duellman, 1970: plate 8), *I. zeteki* (Taylor, 1958), and in most taxa closely related to *Isthmohyla* (*Hyla*, *Smilisca*, *Triprion*, some species of *Tlalocohyla*; e.g., Pope, 1931; Wright, 1931; Pyburn, 1966; Jungfer, 1996; Altig and McDiarmid, 2015). As the phylogenetic position of *I. calypsa* is still unknown, it remains unclear if unpigmented eggs evolved once or twice during the evolutionary history of *Isthmohyla*.

With respect to the size and quantity of ovarian eggs, certain shared characteristics are observed among stream-breeding species of *Isthmohyla*. The female of *I. nacientes* contained mature ovarian eggs of similar size and in comparable quantities (211 eggs, diameter $\bar{x}$ = 2.33 mm; n = 20; this study) to those reported for *I. tica* (190–194 eggs, diameter $\bar{x}$ = 2.32 mm; Starrett, 1966; Lang, 1995). Females of *I. pictipes* (100–149 eggs, diameter $\bar{x}$ = 2.44 mm; Lang, 1995) and *I. rivularis* (76–104 eggs, diameter $\bar{x}$ = 2.33 mm; Lang, 1995) also have similar egg diameters, although they possess fewer ovarian eggs compared to *I. nacientes*.

The presence of *Isthmohyla nacientes* in disturbed environments suggests that this species tolerates relatively disturbed microhabitats, contrary to what is known about other species of *I. tica* species group, which had been reported to inhabit pristine sites (Duellman, 1970, 2001; Savage, 2002; but see Chaves-Acuña et al., 2020). Although further research is needed to understand the potential threats faced by this

species and to identify the factors that enable its survival in these environments, one potential threat is the agricultural expansion of coffee cultivation in recent decades (Cedeño-Fonseca et al., 2020). Coffee crops have gradually encroached upon protected areas of streams and headwaters, consequently exposing these areas to agrochemical pollution and habitat fragmentation (de Jesús Crespo et al., 2020; Montero et al., 2021). This concern is reinforced by recent findings of additional threatened species in this area (*Agalychnis annae* and *Duellmanohyla legleri*; Abarca et al., 2021; Hidalgo-Mora et al., 2021), highlighting the importance of protecting these ecosystems and associated species through conservation programs.

The description of new species plays a pivotal role in laying the groundwork for conservation efforts and targeted conservation strategies (Mace, 2004; Vogel Ely et al., 2017). This becomes particularly crucial in the case of *Isthmohyla*, a group highly vulnerable to habitat loss, climate change, and emerging diseases (Lips 1998, 1999; Lips et al., 2003). Detailed knowledge about species such as *I. nacientes* enhances our understanding of their ecology and reproductive biology, which is vital for the protection of this group of mountainous hylids. Given the specific threats faced by this clade, ongoing research and monitoring are essential to ensure their survival and to implement effective conservation measures.

DATA ACCESSIBILITY

Supplemental material is available at https://www.ichthyologyandherpetology.org/h2024066. Unless an alternative copyright or statement noting that a figure is reprinted from a previous source is noted in a figure caption, the published images and illustrations in this article are licensed by the American Society of Ichthyologists and Herpetologists for use if the use includes a citation to the original source (American Society of Ichthyologists and Herpetologists, the DOI of the *Ichthyology & Herpetology* article, and any individual image credits listed in the figure caption) in accordance with the Creative Commons Attribution CC BY License. ZooBank publication urn:lsid:zoobank.org:pub:E4B8471F-53BE-4585-BBCA-0C74315CA8D3.

AI STATEMENT

The authors declare that no AI-assisted technologies were used in the design and generation of this article and its figures.

ACKNOWLEDGMENTS

We thank T. Calleja, G. Ramírez, G. Ureña, R. Parra, V. Aspinall, Y. Salazar, and the Costa Rica Wildlife Foundation staff for their help during fieldwork. M. O. Pereyra, D. Pereyra, J. Gómez, J. Aquino, S. Barrionuevo, and M. Vallejo helped us in laboratory work. For access to equipment, we thank R. Vargas, M. Springer, and M. Sasa (UCR). We thank R. Ibañez (CH), A. Batista and M. Quiroz (MHCH), A. Sosa (ICGES), and M. Sasa (UCR) for allowing access to the collections under their care; M. Quiroz and A. Batista (MHCH), R. Brown, R. Glor, A. Motta, and C. Meneses (KU), and N. Camacho and G. Pauly (LACM/CRE) for kindly providing photographs of preserved specimens; and G. Ramírez and G. Ureña for sharing photographs of living *Isthmohyla*. E. Moreno reviewed earlier versions of this manuscript. The Cornell Lab of Ornithology kindly made available a free license of Raven Pro software. A. Hertz shared a sound recording of *I. tica* from western Panama.

We thank F. Carbonell for the support from the National System of Conservation Areas (SINAC) and for extending us research permits. This study was conducted under permits SINAC-ACC-PI-re-018-2021, R-SINAC-ACC-PI-re-060-2021, R-SINAC-SE-DT-PI-003-2021, SINAC-SE-PI-LC-132-2023, SINAC-ACC-PI-re-078-2023, CBio-2-2022, and approved by the STRI Animal Care and Use Committee (ACUC; protocol SI-20003). For funding, we thank ANPCYT (PICT 346/2019 and 59/2021), CONICET (PIP2800), FAPESP (Grants #2018/15425-0, CEPID #2021/10639-5), the Pilot Research Grants of the Organization for Tropical Studies (Funds 502, 512, and 521), the Mohamed Bin Zayed Species Conservation Fund (Projects 210526640, 242534066), the Smithsonian Tropical Research Institute Short Term Fellowship (Project 4948), and the Theodore Roosevelt Memorial Fund of the American Museum of Natural History. We thank IDEA WILD for supporting this research.

We thank A. Campos, M. Umaña, F. Mora, E. Monge, F. Cruz, and M. Granados from the Asociación Administradora de los Sistemas de Acueductos y Alcantarillados (ASADA) of San Lorenzo, Tarrazú and R. Parra from Casa Parra Adventures for dedicating so much effort to the conservation of this species and to conserving the water sources where they are found.

Author contributions—WCA: Conceptualization, data curation, formal analysis, funding acquisition, investigation, methodology, project administration, resources, supervision, validation, visualization, writing–original draft, writing–review and editing; JA: Conceptualization, investigation, methodology, project administration, visualization, writing–review and editing; JNP: Conceptualization, investigation, methodology, project administration, visualization, writing–review and editing; EHM: Conceptualization, investigation, methodology, project administration, visualization, writing–review and editing; MUC: Conceptualization, investigation, methodology, project administration, visualization, writing–review and editing; AVC: Conceptualization, investigation, methodology, project administration, visualization, writing–review and editing; GC: Conceptualization, supervision, validation, visualization, writing–review and editing; FB: Conceptualization, supervision, validation, visualization, writing–review and editing; JF: Conceptualization, data curation, formal analysis, funding acquisition, investigation, methodology, project administration, resources, supervision, validation, visualization, writing–original draft, writing–review and editing.

LITERATURE CITED

Abarca, J. G., E. Hidalgo-Mora, R. Ramírez-Campos, and A. Valverde-Castillo. 2021. Predation of a Legler's stream frog, *Duellmanohyla legleri* (Anura: Hylidae), by an ornate cat-eyed snake, *Leptodeira* cf. *ornata* (Squamata: Dipsadidae). Reptiles & Amphibians 28:218–219.

Altig, R., and R. W. McDiarmid. 1999a. Body plan. Development and morphology, p. 24–51. *In*: Tadpoles: The Biology of Anuran Larvae. R. McDiarmid and R. Altig (eds.). The University of Chicago Press, Chicago.

Altig, R., and R. W. McDiarmid. 1999b. Diversity. Familial and generic characterizations, p. 295–337. *In*: Tadpoles: The Biology of Anuran Larvae. R. McDiarmid and R. Altig (eds.). The University of Chicago Press, Chicago.

Altig, R., and R. W. McDiarmid. 2015. Handbook of Larval Amphibians of the United States and Canada. Cornell University Press, Ithaca, New York.

Barrio-Amorós, C. L., C. R. Grünwald, H. Franz-Chávez, A. M. Mendoza, and B. T. La Forest. 2016. Notes on natural history and call description of the Critically Endangered *Plectrohyla avia* (Anura: Hylidae) from Chiapas, Mexico. Amphibian & Reptile Conservation 10:11–17.

Brunetti, A. E., A. Muñoz-Saravia, J. S. Barrionuevo, and S. Reichle. 2017. Silent sounds in the Andes: underwater vocalizations of three frog species with reduced tympanic middle ears (Anura: Telmatobiidae: *Telmatobius*). Canadian Journal of Zoology 95:335–343.

Cedeño-Fonseca, M., M. H. Grayum, T. B. Croat, and M. A. Blanco. 2020. Three new species of *Monstera* (Araceae: Monsteroideae: Monstereae) from the Cordillera de Talamanca in Costa Rica, threatened by the expansion of coffee plantations. Nordic Journal of Botany 38:1–13.

Chaves-Acuña, W., E. Boza-Oviedo, J. Zúniga, G. Chaves, F. Bolaños, C. Vásquez-Almazán, and J. Faivovich. 2024. Phylogenetic relationships of two poorly-known Honduran treefrogs (Hylidae: Hylinae: Hylini). American Museum Novitates 4016:1–17.

Chaves-Acuña, W., T. Calleja, R. Ibañez, M. Quiróz-Espinoza, A. Batista, M. Ponce, A. Hertz, and J. Faivovich. 2025. The tadpole, bioacoustics, natural history, morphological variation, and conservation of *Isthmohyla debilis* (Hylidae: Hylinae: Hylini). Ichthyology & Herpetology 113:625–637.

Chaves-Acuña, W., G. Chaves, J. Klank, E. Arias, F. Bolaños, A. Shepack, T. Leenders, J. Cossel, and J. Faivovich. 2020. Recent findings of *Isthmohyla pictipes* (Anura: Hylidae) in Costa Rica: variation and implications for conservation. Zootaxa 4881:499–514.

de Jesús Crespo, R., T. Douthat, and C. Pringle. 2020. Stream friendly coffee: evaluating the impact of coffee farming on high-elevation streams of the Tarrazú coffee region of Costa Rica. Hydrobiologia 847:1903–1923.

Duellman, W. E. 1970. Hylid frogs of Middle America. Monographs of the Museum of Natural History. University of Kansas, Lawrence, Kansas.

Duellman, W. E. 2001. Hylid Frogs of Middle America. Society for the Study of Amphibians and Reptiles, Ithaca, New York.

Fabrezi, M., and P. Alberch. 1996. The carpal elements of anurans. Herpetologica 52:188–204.

Faivovich, J., C. F. B. Haddad, P. C. A. Garcia, D. R. Frost, J. A. Campbell, and W. C. Wheeler. 2005. Systematic review of the frog family Hylidae, with special reference to Hylinae: phylogenetic analysis and taxonomic revision. Bulletin of the American Museum of Natural History 294:1–240.

Faivovich, J., M. O. Pereyra, M. C. Luna, A. Hertz, B. Blotto, C. R. Vásquez-Almazán, J. R. McCranie, D. Sanchez-Ramirez, D. Baêta, K. Araujo-Vieira, G. Köhler, B. Kubicki, J. A. Campbell, D. R. Frost, and C. F. B. Haddad. 2018. The monophyly and relationships of several genera of Hylinae (Anura: Hylidae: Hylinae) with comments on recent taxonomic changes in hylids. South American Journal of Herpetology 13:1–32.

Farris, J. S., V. A. Albert, M. Källersjo, D. Lipscomb, and A. G. Kluge. 1996. Parsimony jackknifing outperforms neighbor-joining. Cladistics 12:99–124.

Frost, D. R. 2026. Amphibian Species of the World: an online reference, version 6.2 (1 May 2026). Electronic database accessible at https://amphibiansoftheworld.amnh.org/index.php. American Museum of Natural History.

Goloboff, P. A. 1999. Analyzing large datasets in reasonable times: solutions for composite optima. Cladistics 15:415–428.

Goloboff, P. A., and M. F. Morales. 2023. TNT version 1.6, with a graphical interface for MacOS and Linux, including new routines in parallel. Cladistics 39:144–153.

Gosner, K. L. 1960. A simplified table for staging anuran embryos and larvae with notes on identification. Herpetologica 16:183–190.

Grosjean, S. 2005. The choice of external morphological characters and developmental stages for tadpole-based anuran taxonomy: a case study in *Rana (Sylvirana) nigrovittata* (Blyth, 1855) (Amphibia, Anura, Ranidae). Contributions to Zoology 74:61–76.

Hall, T. A. 1999. BioEdit: a user-friendly biological sequence alignment editor and analysis program for Windows 95/98/NT. Nucleic Acids Symposium Series 41:95–98.

Hidalgo-Mora, E., J. Navarro-Picado, and J. G. Abarca. 2022. Notes on geographic distribution, advertisement call and habitat of the Starrett's tree frog *Isthmohyla tica* (Hylidae) in the Zona de los Santos, Costa Rica. Revista Latinoamericana de Herpetología 5:112–120.

Hidalgo-Mora, E., A. Valverde-Castillo, and J. G. Abarca. 2021. Range extension of the blue-sided leaf frog, *Agalychnis annae* (Anura: Hylidae): using citizen science across suburban areas in Costa Rica. Reptiles & Amphibians 28:264–267.

Hoang, D. T., O. Chernomor, A. von Haeseler, B. Q. Minh, and L. S. Vinh. 2018. UFBoot2: improving the ultrafast bootstrap approximation. Molecular Biology and Evolution 35:518–522.

Ibáñez, D. R., and E. M. Smith. 1995. Systematic status of *Colosthetus flotator* and *C. nubicola* (Anura: Dendrobatidae) in Panama. Copeia 1995:446–456.

Jungfer, K. H. 1996. Reproduction and parental care of the coronated treefrog, *Anotheca spinosa*. Herpetologica 52:25–32.

Kalyaanamoorthy, S., B. Q. Minh, T. K. Wong, A. von Haeseler, and L. S. Jermiin. 2017. ModelFinder: fast model selection for accurate phylogenetic estimates. Nature Methods 14:587–589.

Katoh, K., and D. M. Standley. 2013. MAFFT multiple sequence alignment software version7: improvements in performance utility. Molecular Biology and Evolution 30:772–780.

Köhler, J., M. Jansen, A. Rodríguez, P. J. R. Kok, L. F. Toledo, M. Emmrich, F. Glaw, C. F. B. Haddad, M. O. Rödel, and M. Vences. 2017. The use of bioacoustics in anuran taxonomy: theory, terminology, methods and recommendations for best practice. Zootaxa 4251:1–124.

Lang, C. 1995. Size-fecundity relationships among stream-breeding hylid frogs. Herpetological Natural History 3:193–197.

Lavilla, E. O., and G. J. Scrocchi. 1986. Morfometría larval de los géneros de Telmatobiinae (Anura, Leptodactylidae) de Argentina y Chile. Physis 44:39–43.

Lins, A. C. R., R. F. De Magalhaes, R. N. Costa, R. A. Brandao, T. R. Py-Daniel, N. E. De Oliveira Miranda, N. M. Maciel, F. Nomura, and T. L. Pezzuti. 2018. The larvae of two species of *Bokermannohyla* (Anura, Hylidae, Cophomantini) endemic to the highlands of central Brazil. Zootaxa 4527:5019–5520.

Lips, K. R. 1996. New treefrog from the Cordillera de Talamanca of Central America with a discussion of systematic relationships in the *Hyla lancasteri* group. Copeia 1996:615–626.

Lips, K. R. 1998. Decline of a tropical montane amphibian fauna. Conservation Biology 12:106–117.

Lips, K. R. 1999. Mass mortality and population declines of anurans at an upland site in western Panama. Conservation Biology 13:117–125.

Lips, K. R., D. E. Green, and R. Papendick. 2003. Chytridiomycosis in wild frogs from southern Costa Rica. Journal of Herpetology 37:215–218.

Lizana, M., R. Márquez, and R. Martín-Sánchez. 1994. Reproductive biology of *Pelobates cultripes* (Anura: Pelobatidae) in central Spain. Journal of Herpetology 28:19–27.

Luna, M. C., R. W. McDiarmid, and J. Faivovich. 2018. From erotic excrescences to pheromone shots: structure and diversity of nuptial pads in anurans. Biological Journal of the Linnean Society 124:403–446.

Lynch, J., and W. E. Duellman. 1980. The *Eleutherodactylus* of the Amazonian slopes of the Ecuadorian Andes (Anura: Leptodactylidae). University of Kansas, Museum of Natural History, Miscellaneous Publication 69:1–86.

Mace, G. 2004. The role of taxonomy in species conservation. Philosophical Transactions of the Royal Society B: Biological Sciences 359:711–719.

McDiarmid, R. W., and R. Altig. 1999. Tadpoles: The Biology of Anuran Larvae. The University of Chicago Press, Chicago.

Minh, B. Q., M. A. T. Nguyen, and A. von Haeseler. 2013. Ultrafast approximation for phylogenetic bootstrap. Molecular Biology and Evolution 305:1188–1195.

Montero, A., J. Marull, E. Tello, C. Cattaneo, F. Coll, M. Pons, J. Infante-Amate, A. Urrego-Mesa, A. Fernández-Landa, and M. Vargas. 2021. The impacts of agricultural and urban land-use changes on plant and bird biodiversity in Costa Rica (1986–2014). Regional Environmental Change 21:48.

Myers, C. W., and W. E. Duellman. 1982. A new species of *Hyla* from Cerro Colorado, and other tree frog records and geographical notes from western Panama. American Museum Novitates 2752:1–32.

Napoli, M. F., and U. Caramaschi. 1998. Duas novas especies de *Hyla* Laurenti, 1768 do Brasil Central afins de *H. tritaeniata* Bokermann, 1965 (Amphibia, Anura, Hylidae). Boletim do Museo Nacional, Nova Serie, Zoologia 391:1–12.

Nguyen, L. T., H. A. Schmidt, A. von Haeseler, and B. Q. Minh. 2015. IQ-TREE: a fast and effective stochastic algorithm for estimating maximum-likelihood phylogenies. Molecular Biology and Evolution 321:268–274.

Nixon, K. C. 1999. The parsimony ratchet, a new method for rapid parsimony analysis. Cladistics 15:407–414.

Pezzuti, T. L., F. S. F. Leite, D. de C. Rossa-Feres, and P. C. A. Garcia. 2021. The tadpoles of the Iron Quadrangle, southeastern Brazil: a baseline for larval knowledge and anuran conservation in a diverse and threaten region. South American Journal of Herpetology 22(sp1):1–107.

Pope, C. H. 1931. Notes on the amphibians from Fukien, Hainan, and other parts of China. Bulletin of the American Museum of Natural History 61:397–611.

Pyburn, W. F. 1966. Breeding activity, larvae and relationships of the treefrog *Hyla phaeota cyanosticta*. The Southwestern Naturalist 11:1–18.

R Core Team. 2020. R: a language and environment for statistical computing. R Foundation for Statistical Computing, Vienna, Austria. https://www.R-project.org/

Rambaut, A. 2014. FigTree, tree figure drawing tool, Version 1.4.2. https://tree.bio.ed.ac.uk/software/figtree/

Savage, J. M. 2002. The Amphibians and Reptiles of Costa Rica: A Herpetofauna Between Two Continents, Between Two Seas. The University of Chicago Press, Chicago.

Savage, J. M., and W. R. Heyer. 1967. Variation and distribution in the tree-frog genus *Phyllomedusa* in Costa Rica, Central America. Beitrage zur Neotropischen Fauna 5:111–131.

Savage, J. M., and W. R. Heyer. 1969. The tree-frogs (family Hylidae) of Costa Rica: diagnosis and distribution. Revista de Biología Tropical 16:1–127.

Smith, S. A., S. Arif, A. N. M. de Oca, and J. J. Wiens. 2007a. A phylogenetic hot spot for evolutionary novelty in Middle American treefrogs. Evolution 61:2075–2085.

Smith, S. A., A. N. M. de Oca, T. W. Reeder, and J. J. Wiens. 2007b. A phylogenetic perspective on elevational species richness patterns in Middle American treefrogs: why so few species in lowland tropical rainforests? Evolution 61:1188–1207.

Starrett, P. 1966. Rediscovery of *Hyla pictipes* Cope, with description of a new montane stream *Hyla* from Costa Rica. Bulletin of the Southern California Academy of Sciences 65:17–28.

Sueur, J., T. Aubin, and C. Simonis. 2008. Seewave, a free modular tool for sound analysis and synthesis. Bioacoustics 18:213–226.

Taylor, E. H. 1958. Additions to the known herpetofauna of Costa Rica with comments on other species. No. III. University of Kansas Science Bulletin 39:3–40.

Trueb, L. 1968. Variation in the tree frog *Hyla lancasteri*. Copeia 1968:285–299.

Vaidya, G., D. J. Lohman, and R. Meier. 2011. SequenceMatrix: concatenation software for the fast assembly of multi-gene datasets with character set and codon information. Cladistics 27:171–180.

Vogel Ely, C., S. A. d. L. Bordignon, R. Trevisan, and I. I. Boldrini. 2017. Implications of poor taxonomy in conservation. Journal for Nature Conservation 36:10–13.

Watters, J. L., S. T. Cummings, R. L. Flanagan, and C. D. Siler. 2016. Review of morphometric measurements used in anuran species descriptions and recommendations for a standardized approach. Zootaxa 4072:477–495.

Wiens, J. J., J. W. Fetzner Jr., C. L. Parkinson, and T. W. Reeder. 2005. Hylid frog phylogeny and sampling strategies for speciose clades. Systematic Biology 54:719–748.

Wiens, J. J., C. A. Kuczynski, X. Hua, and D. S. Moen. 2010. An expanded phylogeny of treefrogs (Hylidae) based on nuclear and mitochondrial sequence data. Molecular Phylogenetics and Evolution 55:871–882.

Wright, A. H. 1931. Life-histories of the Frogs of Okefinokee Swamp, Georgia. Macmillan, New York.

Zheng, Y. 2019. The co-occurrence of loose skin and underwater calling in frogs–further evidence from *Amolops rickettui* and its implications. Journal of Zoology 309:280–286.

Zheng, Y., D. Rao, R. W. Murphy, and X. Zeng. 2011. Reproductive behavior and underwater calls in the Emei mustache toad, *Leptobrachium boringii*. Asian Herpetological Research 2:199–215.